MRC mission research corporation

WILDLAND FIRE MODELING FOR PLANNING SUPPORT

VOLUME IV -- RATE OF SPREAD MODEL ASSESSMENT

MRC Report No. 7611-3-876

Submitted to:

USDA Forest Service
Contract No. 21-393

Submitted by:

Mission Research Corporation
P.O. Drawer 719
Santa Barbara, CA 93102

Prepared by:

J. C. Sanderlin
J. M. Sunderson

August 1976

TABLE OF CONTENTS

VOLUME IV

1.0	INTRODUCTION	1
2.0	OBJECTIVES OF SENSITIVITY ANALYSIS	1
3.0	PROCEDURE	1
	3.1 CASES CONSIDERED	6
4.0	RESULTS	6
5.0	CONCLUSIONS	10

LIST OF TABLES

Table 1	ROS Model Input Parameters	2
Table 2	ROS Model Input Parameters, Weak and Strong Variables	4
Table 3	Values of ROS Model Variables	5
Table 4	Cases Examined	7
Table 5	Characteristics Summary	8
Table 6	Brief Characteristics Summary	11

LIST OF FIGURES

Figure 1	Probability Density of $(R/\overline{R})$ for Variation of W_o.	15
Figure 2	Cumulative Probability Distribution of $(R/\overline{R})$ for Variation of W_o.	16
Figure 3	Probability Density of $(R/\overline{R})$ for Variation of h.	17
Figure 4	Cumulative Probability Distribution of $(R/\overline{R})$ for Variation of h.	18
Figure 5	Probability Density of $(R/\overline{R})$ for Variation of ρ_p.	19
Figure 6	Cumulative Probability Distribution of $(R/\overline{R})$ for Variation of ρ_p.	20
Figure 7	Probability Density of $(R/\overline{R})$ for Variation of S_T.	21
Figure 8	Cumulative Probability Distribution of $(R/\overline{R})$ for Variation of S_T.	22
Figure 9	Probability Density of $(R/\overline{R})$ for Variation of S_E.	23
Figure 10	Cumulative Probability Distribution of $(R/\overline{R})$ for Variation of S_E.	24
Figure 11	Probability Density of $(R/\overline{R})$ for Variation of $\tan\phi$.	25
Figure 12	Cumulative Probability Distribution of $(R/\overline{R})$ for Variation of $\tan\phi$.	26
Figure 13	Probability Density of $(R/\overline{R})$ for Variation of u.	27
Figure 14	Cumulative Probability Distribution of $(R/\overline{R})$ for Variation of u.	28
Figure 15	Probability Density of $(R/\overline{R})$ for Variation of σ.	29
Figure 16	Cumulative Probability Distribution of $(R/\overline{R})$ for Variation of σ.	30
Figure 17	Probability Density of $(R/\overline{R})$ for Variation of δ.	31

LIST OF FIGURES

Figure 1	Probability Density of $(R/\overline{R})$ for Variation of W_o.	15
Figure 2	Cumulative Probability Distribution of $(R/\overline{R})$ for Variation of W_o.	16
Figure 3	Probability Density of $(R/\overline{R})$ for Variation of h.	17
Figure 4	Cumulative Probability Distribution of $(R/\overline{R})$ for Variation of h.	18
Figure 5	Probability Density of $(R/\overline{R})$ for Variation of ρ_p.	19
Figure 6	Cumulative Probability Distribution of $(R/\overline{R})$ for Variation of ρ_p.	20
Figure 7	Probability Density of $(R/\overline{R})$ for Variation of S_T.	21
Figure 8	Cumulative Probability Distribution of $(R/\overline{R})$ for Variation of S_T.	22
Figure 9	Probability Density of $(R/\overline{R})$ for Variation of S_E.	23
Figure 10	Cumulative Probability Distribution of $(R/\overline{R})$ for Variation of S_E.	24
Figure 11	Probability Density of $(R/\overline{R})$ for Variation of $\tan\phi$.	25
Figure 12	Cumulative Probability Distribution of $(R/\overline{R})$ for Variation of $\tan\phi$.	26
Figure 13	Probability Density of $(R/\overline{R})$ for Variation of u.	27
Figure 14	Cumulative Probability Distribution of $(R/\overline{R})$ for Variation of u.	28
Figure 15	Probability Density of $(R/\overline{R})$ for Variation of σ.	29
Figure 16	Cumulative Probability Distribution of $(R/\overline{R})$ for Variation of σ.	30
Figure 17	Probability Density of $(R/\overline{R})$ for Variation of δ.	31

LIST OF FIGURES (CONTINUED)

Figure 18	Cumulative Probability Distribution of $(R/\overline{R})$ for Variation of δ.	32
Figure 19	Probability Density of $(R/\overline{R})$ for Variation of M_f.	33
Figure 20	Cumulative Probability Distribution of $(R/\overline{R})$ for Variation of M_f.	34
Figure 21	Probability Density of $(R/\overline{R})$ for Variation of M_x.	35
Figure 22	Cumulative Probability Distribution of $(R/\overline{R})$ for Variation of M_x.	36
Figure 23	Probability Density of $(R/\overline{R})$ for Variation of u,σ.	37
Figure 24	Cumulative Probability Distribution of $(R/\overline{R})$ for Variation of u,σ.	38
Figure 25	Probability Density of $(R/\overline{R})$ for Variation of u,δ.	39
Figure 26	Cumulative Probability Distribution of $(R/\overline{R})$ for Variation of u,δ.	40
Figure 27	Probability Density of $(R/\overline{R})$ for Variation of σ,δ.	41
Figure 28	Cumulative Probability Distribution of $(R/\overline{R})$ for Variation of σ,δ.	42
Figure 29	Probability Density of $(R/\overline{R})$ for Variation of u,σ,δ.	43
Figure 30	Cumulative Probability Distribution of $(R/\overline{R})$ for Variation of u,σ,δ.	44
Figure 31	Probability Density of $(R/\overline{R})$ for Variation of M_f,M_x.	45
Figure 32	Cumulative Probability Distribution of $(R/\overline{R})$ for Variation of M_f,M_x.	46
Figure 33	Probability Density of $(R/\overline{R})$ for Variation of All Weak Variables.	47

LIST OF FIGURES (CONTINUED)

Figure 34	Cumulative Probability Distribution of $(R/\overline{R})$ for Variation of All Weak Variables.	48
Figure 35	Probability Density of $(R/\overline{R})$ for Variation of All Strong Variables.	49
Figure 36	Cumulative Probability Distribution of $(R/\overline{R})$ for Variation of All Strong Variables.	50
Figure 37	Probability Density of $(R/\overline{R})$ for Variation of All Variables.	51
Figure 38	Cumulative Probability Distribution of $(R/\overline{R})$ for Variation of All Variables.	52

1.0 INTRODUCTION

A preliminary sensitivity analysis of the rate of spread model[1] considered the effect upon estimated spread rate of uncertainties in each variable independent of uncertainties in any other variable. This study identified six variables as weakly affecting estimated spread rate and five variables as strongly affecting estimated spread rate. It was suggested that a coupled-variable analysis of weak-and-weak variables would probably produce weak results, a coupled-variable analysis of weak-and-strong variables would probably be dominated by the strong variable and a coupled-variable analysis of strong-and-strong variables might affect estimated spread rate more strongly than either variable alone.

2.0 OBJECTIVES OF SENSITIVITY ANALYSIS

The objective of the current analysis of ROS model sensitivity is to examine the coupled effects of uncertainties due to combinations of the strong variables upon estimated spread rate. In addition, it is of interest to provide a methodology capable of either providing an indication of estimated spread rate uncertainty for specified uncertainties in the spread rate model variables, or conversely, of providing an indication of tolerable uncertainties in the spread rate model variables for specified uncertainty in estimated spread rates.

3.0 PROCEDURE

Spread rate (R) as estimated by the ROS model[2] is a function of a set of variables (q_i) of the form[1]:

$$R = f(q_1, q_2, \ldots, q_n) \qquad (1)$$

where the q_i variables are defined in Table 1. Partition the set of variables q_i into a subset of weak variables W_i and strong variables S_i to obtain

Table 1

ROS Model Input Parameters

Input Parameters for Basic Equations

w_o, ovendry fuel loading, lb./ft.^{2}

δ, fuel depth, ft.

σ, fuel particle surface-area-to-volume ratio, 1/ft.

h, fuel particle low heat content, B.t.u./lb.

ρ_p, ovendry particle density, lb./ft.^{3}

M_f, fuel particle moisture content, $\frac{\text{lb. moisture}}{\text{lb. ovendry wood}}$

S_T, fuel particle total mineral content, $\frac{\text{lb. minerals}}{\text{lb. ovendry wood}}$

S_e, fuel particle effective mineral content, $\frac{\text{lb. silica-free minerals}}{\text{lb. ovendry wood}}$

U, wind velocity at midflame height, ft./min.

$\tan \phi$, slope, vertical rise/horizontal distance

M_x, moisture content of extinction. This term needs experimental determination. We are presently using 0.30, the fiber saturation point of many dead fuels. For aerial fuels (β <.02) with low wind velocity (<5 m.p.h.) $M_x \simeq 0.15$.

$$R = f(W_1, W_2, \ldots, W_m, S_1, S_2, \ldots, S_n) \qquad (2)$$

where the weak and strong variables are identified in Table 2. To investigate the effects upon spread rate of combined uncertainties in the five strong variables of Table 2 requires examination of all the combinations of these variables together with examination of all the combinations of values that may be assumed by each combination of variables. Straightforward calculation of all the pertinent spread rates involves a lengthy, but manageable, computation process; however, presentation of the resulting spread rate uncertainties as a function of the several variables is difficult. A statistical procedure employed here provides an organization for the required computations as well as a compact presentation of the results.

For each ROS model variable (q_i) define a normally distributed probability density function G_i having mean $\overline{q}_i$ and standard deviation $1.4826(PE)_i$ where $\overline{q}_i$ is the average value of q_i and $(PE)_i$ is the probable error in q_i shown in Table 3. Any combination of variables q_j, q_k, q_l of (1) can now be replaced by variables g_j, g_k, g_l obtained from G_j, G_k, G_l by random selection. An ensemble of N such spread rate calculations provides a discrete representation of the probability density function for spread rate resulting from random variation of the selected combination of variables.

For presentation purposes it is convenient to normalize spread rate to an average value ($\overline{R}$) defined by

$$\overline{R} = f(\overline{q}_1, \overline{q}_2, \ldots, \overline{q}_n) \ , \qquad (3)$$

where the average values of $\overline{q}_i$ are shown in Table 3, and to normalize frequency per interval to the maximum frequency occurrence. The results are thus of the form:

Table 2. ROS Model Input Parameters, Weak and Strong Variables

Weak Variables

w_o - ovendry fuel loading

h - fuel particle low heat content

ρ_p - ovendry particle density

S_T - fuel particle total mineral content

S_e - fuel particle silica-free mineral content

tan ϕ - slope

Strong Variables

U - wind speed at midflame height

σ - fuel particle surface-area-to-volume ratio

δ - fuel depth

M_f - fuel particle moisture fraction

M_x - moisture content of extinction

Table 3. Values of ROS Model Variables[1]

Weak Variables

Variable	Units	Minimum Value	Average Value	Maximum Value	Probable Error Percent	Standard Deviation
W_o	lb/ft^2	0.034	0.20	0.368	20	0.045
h	Btu/lb	6480.0	7830.8	9180.0	10	580.5
ρ_p	lb/ft^3	18.7	29.7	40.6	10	4.4
S_T	--	0.0016	0.081	0.16	20	0.024
S_e	--	0.0005	0.025	0.05	20	0.007
tan ϕ	--	0.01	1.0	2.0	10	0.15
		Strong Variables				
U	ft/min	35.2	1776.0	3520.0	40	1054.2
σ	1/ft	300.0	1900.0	3500.0	15	422.5
δ	ft	1.0	3.5	6.0	10	0.52
M_f	--	0.03	0.115	0.2	40	0.068
M_x	--	0.18	0.29	0.4	30	0.13

(1) Sanderlin, J.C. and Sunderson, J.M., op. cit.

$$n_j/n_m = f(R_i/\overline{R}) \qquad (4)$$

where

n_j = the number of values of $R/\overline{R}$ occurring in the j-th interval

n_m = the number of values of $R/\overline{R}$ in the ensemble.

3.1 CASES CONSIDERED

Examination of the ROS Model equation[2] shows that the moisture related variables M_f, M_x are clearly decoupled from the variables u,σ,δ. Thus the only combinations of variables that need to be considered for a coupled-variable analysis of the strong variables are (u,σ). (u,δ), (σ,δ), (M_f,M_x) and $(u,\sigma,\delta,M_f,M_x)$. since the independent effects of each variable have been previously considered.[1]

In addition to considering the above combinations of the strong variables, three additional cases were examined to relate the current work with previous work.[1] These cases are (1) each independent variable, (2) all weak variables simultaneously and (3) all variables simultaneously.

4.0 RESULTS

The probability density and cumulative probability distribution of R/R were obtained for normal distributions of the spread rate variables with the means and standard deviations shown in Table 3. The cases that were examined and the respective figure numbers are listed in Table 4, where the probability density functions are shown in the odd numbered figures and the cumulative probability distributions are shown in the even numbered figures. The results of Figures 1 through 38 are summarized in Table 5 in terms of the

Table 4. Cases Examined

Case	Inclusive Figure Numbers
Each weak variable individually	1-12
Each strong variable individually	13-22
Simultaneous combinations of strong variables	23-32
All weak variables simultaneously	33-34
All strong variables simultaneously	35-36
All variables simultaneously	37-38

Table 5. Characteristics Summary

CASE	MEAN ($R/\bar{R}$)	MODE ($\tilde{R/\bar{R}}$)	STD. DEV. $\sigma R/\bar{R}$	80% CONF. LIMITS $R/\bar{R}$ (10)	80% CONF. LIMITS $R/\bar{R}$ (90)	FIGURE NOS. Density/Distribution
			WEAK VARIABLES			
W_o	1.00	1.00	0.01	0.99	1.01	1/2
h	1.00	1.02	0.07	0.89	1.09	3/4
ρ_p	1.00	1.00	0.007	0.99	1.01	5/6
S_T	1.00	0.99	0.02	0.97	1.03	7/8
S_e	1.01	0.99	0.07	0.93	1.08	9/10
tan ϕ	1.00	1.01	0.05	0.94	1.06	11/12
			STRONG VARIABLES			
u	1.18	0.74	0.68	0.30	2.01	13/14
σ	1.06	1.12	0.42	0.49	1.56	15/16
δ	1.00	1.03	0.15	0.78	1.18	17/18
M_f	1.07	0.93	0.40	0.63	1.52	19/20
M_x	0.99	1.00	0.14	0.88	1.07	21/22
			COUPLED STRONG VARIABLES			
u,σ	1.22	0.38	0.91	0.26	2.45	23/24
u,δ	0.96	1.11	0.56	0.23	1.76	25/26
σ δ	1.06	0.96	0.45	0.46	1.69	27/28
u,σ, δ	1.24	0.32	0.97	0.19	2.52	29/30
M_f, M_x	1.10	0.94	0.43	0.67	1.66	31/32
			COUPLED STRONG, WEAK AND ALL VARIABLES			
All Weak	1.03	1.01	0.11	0.86	1.14	33/34
All Strong	1.34	0.34	1.28	0.12	2.89	35/36
All Variables	1.29	0.62	1.13	0.16	2.99	37/38

mean, mode, standard deviation and eighty percent confidence interval of the resulting distributions of R/R.

The probability density functions of $R/\overline{R}$ for variation of the weak variables are characterized by means of R/R=1.0, modes of $R/\overline{R} \simeq 1.0$ and standard deviations of $\sigma_{R/\overline{R}} < 0.1$. The most effective weak variable is fuel particle silica-free mineral content (S_E) with a standard deviation of 0.07 and an 80 percent confidence variation in $R/\overline{R}$ of about ± 10 percent.

With the exception of windspeed at midflame height, the probability density functions of R/R for variation of the strong variables are characterized by means of $R/\overline{R} \simeq 1.0$, modes of $R/\overline{R} \simeq 1.0$ and standard deviations of $\sigma_{R/\overline{R}} > 0.1$. The mean of the density for windspeed variation is 18 percent above the expected value while the mode is 26 percent less than the expected value. It will be observed in all but one case where u is a variable that the mode is shifted to a value less than 1.0. The reason for this shift is that the average fuel characteristics used are such that spread rate is reaction intensity limited[2] so that large increases in wind speed are not accompanied by increases in spread rate, although large decreases in wind speed are accompanied by significant decreases in spread rate. Windspeed is clearly the strongest of the spread rate model variables with a standard deviation of 0.68, and an 80 percent confidence interval from $R/\overline{R} = 0.3$ to $R/\overline{R} = 2.01$.

The probability density functions of $R/\overline{R}$ for simultaneous variation of the strong variables are strong functions of the particular variables involved. The mean values are within 25 percent of 1.0, being generally greater than 1.0 for cases where δ is varied. The modes are generally about 1.0, except in cases where u and δ are simultaneously varied, for which the modes are approximately 0.35. The strongest combination of strong variables is u,δ, and σ with a standard deviation of $\sigma_{R/\overline{R}} = 0.97$ and an 80 percent confidence interval from $R/\overline{R} = 0.19$ to $R/R = 2.52$; however, it is significant that the variables u and σ are responsible for about 95 percent of this variation in $R/\overline{R}$. The probability density function of R/R for simultaneous variation of

M_F and M_x is essentially dominated by M_f. This is to be expected for values of M_x such that R>0, and only these values of M_x were considered.

Simultaneous variation of all weak variables produces weak effects, and simultaneous variation of all strong variables produces strong effects. Simultaneous variation of all variables produces a slightly smaller standard deviation than simultaneous variation than of all strong variables; however, considering the magnitude of the effect of the weak variables, this anomaly is not considered significant.

5.0 CONCLUSIONS

An objective of the FIRESCOPE program is to determine the potential utility of wildland fire perimeter prediction in real time operational planning support of suppression activities. Of key importance in wildland fire perimeter prediction is the estimate of local spread rate in wildland fuels at all points of interest. The data requirements of the spread rate model are considerable, and particularly significant since much of these data must be collected from the field at high resolution (approximately 100 meters), and over an extensive land area. Allowable data uncertainties in terms of acceptable fire perimeter prediction errors as defined by acceptable deviations of local spread rate values from reality can significantly affect the resolution, accuracy and thus the quality and quantity of the contents of the potentially large data set required to provide an acceptable level of performance.

The complete set of input variables required by the spread rate model are shown in Table I. It will be recalled that the results presented in Figures 1 through 38 are based on parameter variations over normally distributed probable error distributions based on slightly conservative (i.e., large) estimates of probable error. Thus, the deviations presented in those figures are larger than would be expected in any normal real situation.

Table 6 presents a brief summary of Table 5 based on the relative widths of the 80 percent confidence intervals for a selected set of variables. Since the weak variables constitute at most a 10 percent deviation of spread rate

Table 6. Brief Characteristics Summary

Case	Relative Width of 80% Confidence Interval (Percent)
All Weak	10
M_f	31
σ	38
u	60
u, σ	77
u, σ, δ	82
All Strong	98
All	100

relative to the expected value, none of these variables can be considered of primary significance. The primary variables in order of importance are wind velocity ($u\hat{a}_u$), fuel particle volume to area ratio (σ), fuel particle moisture fraction (M_f) and of significantly lesser sensitivity fuel depth (δ) and moisture of extinction (M_x).

Based upon the foregoing discussion, the following conclusions are presented.

- Fuel loading (W_o) and fuel depth (δ) can be safely modeled for a limited set of fuel types as a function of fuel age. A detailed accounting of site dependent variables (e.g., soil type, moisture availability, slope, aspect, etc.) is probably not necessary, although inclusion of order-of-magnitude effects may be beneficial.

- The 80 percent confidence interval of slopes ranging from -65 to +65 degrees is only about 5 percent of the 80 percent confidence interval for all variables. Slope can thus be quantized over 4 to 6 intervals between -90 degrees and +90 degrees for computation of the slope function ϕ_w^2.

- Fuel particle low heat content (h). oven-dry fuel particle density (ρ_p) together with fuel particle silica-free (S_E) and total (S_T) mineral content can be treated as constants, possibly quantized by fuel type and site dependent conditions.

- The moisture content of extinction (M_x) forms, together with fuel particle moisture fraction (M_f) a switching function which determines primarily whether or not the fuel will burn, with a generally second order effect upon spread rate. Laboratory specification should be possible for constant values of M_x by fuel type, possibly quantized as a function of fuel size class and type.

- Fuel particle area-to-volume ratio (σ) can be best specified by laboratory analysis of representative samples of the fuel types of interest. It will be necessary to define average values of σ over selected fuel particle size classes, and possibly quantized as a function of fuel age.

- Windspeed is clearly the dominant variable in the spread rate model. For perimeter prediction purposes, direction of spread is equally important. Thus wind velocity $\vec{u} = u\hat{a}_u$ is the variable of interest. Wind velocity probably has the greatest dynamic range, and certainly exhibits the most dynamic variability of the spread rate model variables. Because of spatial variations wind velocity must be modeled as a function of location. Because of temporal variations as a function of location these models must exhibit, at least limited (i.e., 1-2 hours) and ideally long term (i.e., 12-24 hours) predictive capabilities. Further, the spatial resolution of calculated wind velocity data are dictated by the sensitivity of wind velocity to location and the sensitivity of perimeter growth to wind velocity, which are both large. Topography data requirements are specified by terrain effects for wind modeling, and not by slope effects on spread rate. Topographical data should concentrate upon definition of ridge lines and drainage patterns. Resolution requirements are uncertain; however, a horizontal resolution of 200 feet is probably generally adequate, with perhaps somewhat smaller values in extremely convoluted terrain. Fine scale wind velocity models with limited predictive capability are in development. The accuracy of these models under meteorological conditions of primary interest to wildland fire suppression has not been determined. Work has not begun on fine scale wind models with long term predictive capability.

- Fuel moisture must be specified for both live and dead fuels. Live fuel moisture depends primarily upon ground moisture availability and plant utilization of moisture. It should be adequate to develop a seasonal live fuel moisture model as a function of available moisture and fuel type for a specified set of fuel particle size classes.

- Dead fuels are hygroscopic and their time constants are sensitive functions of fuel particle size. Laboratory analysis should be able to produce data for empirical models of dead fuel moisture content as a function of temperature, humidity and windspeed for specified size classes of the fuel types of interest. It should be noted that dead fuel moisture content is extremely dependent upon windspeed through drying rate.

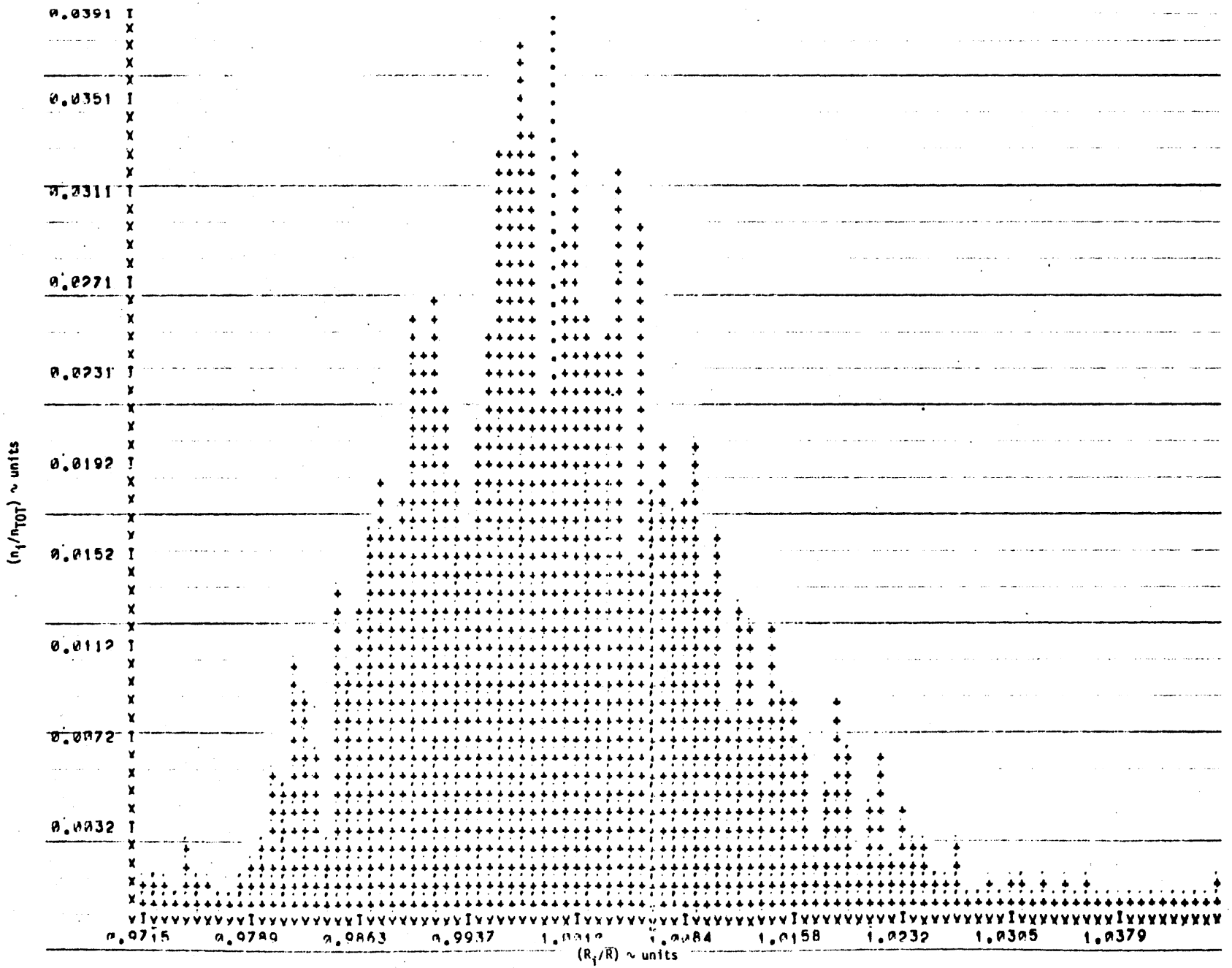

Figure 1. Probability Density of $(R/\bar{R})$ for Variation of W_o.

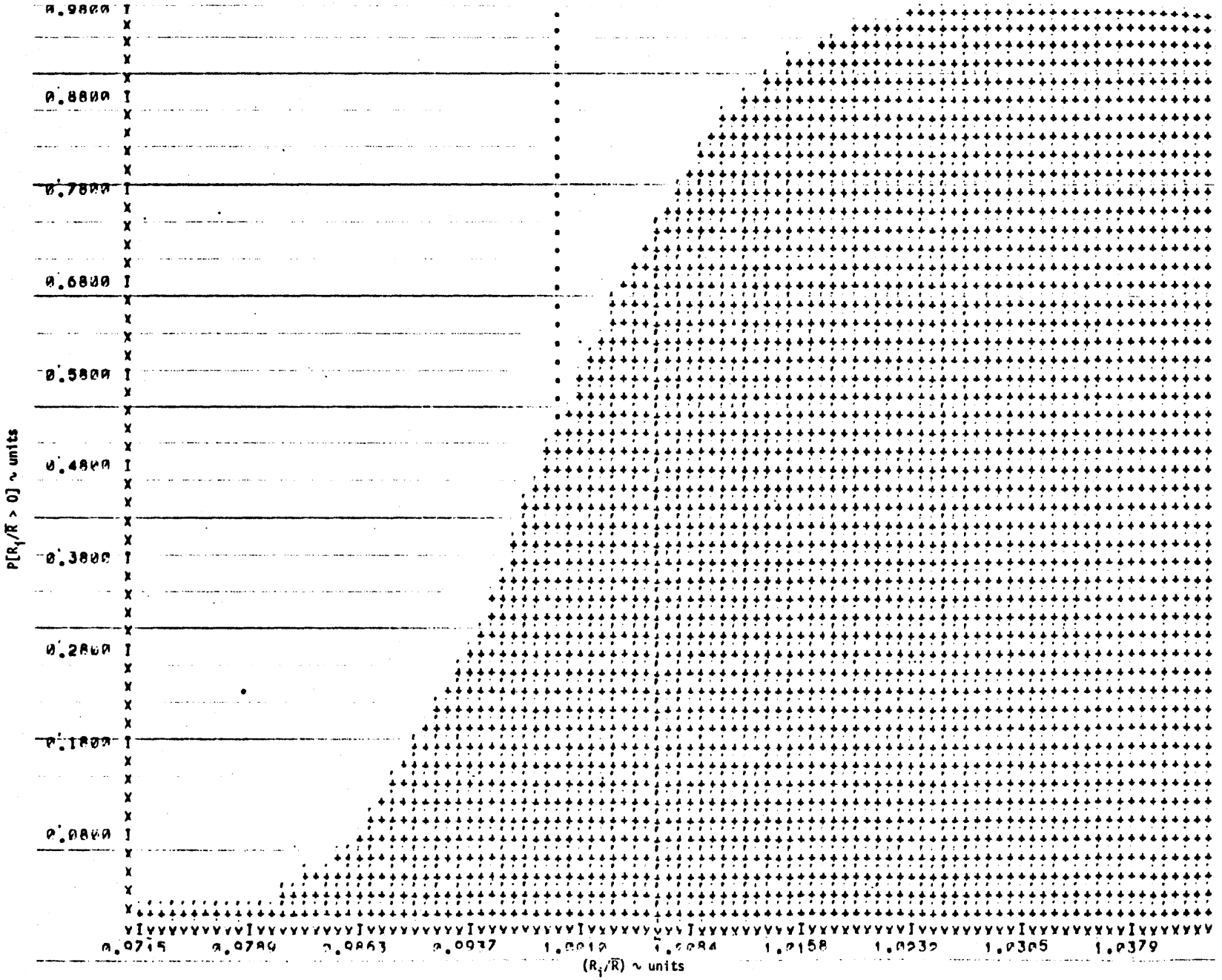

Figure 2. Cumulative Probability Distribution of $(R/\overline{R})$ for Variation of W_o.

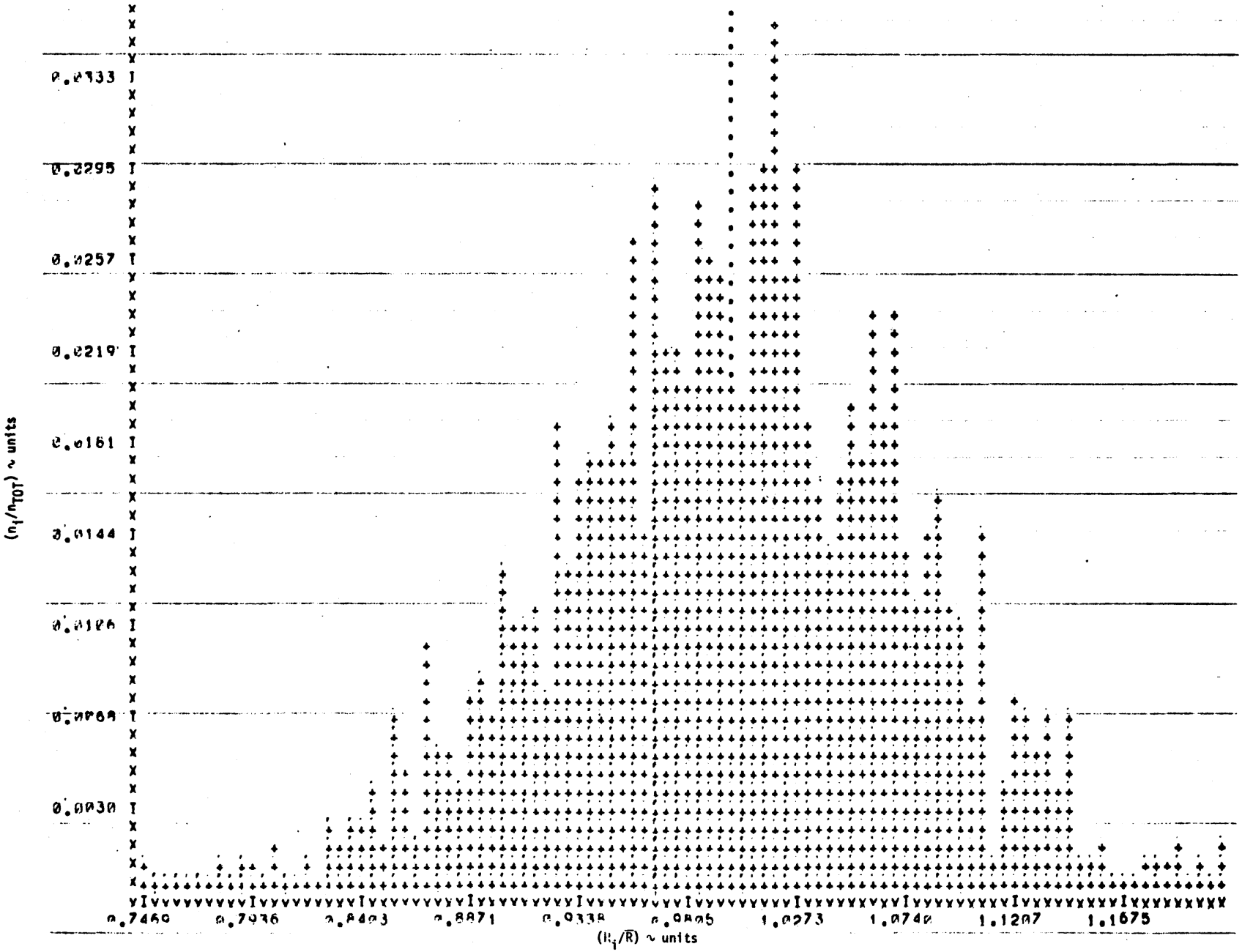

Figure 3. Probability Density of $(R/\overline{R})$ for Variation of h.

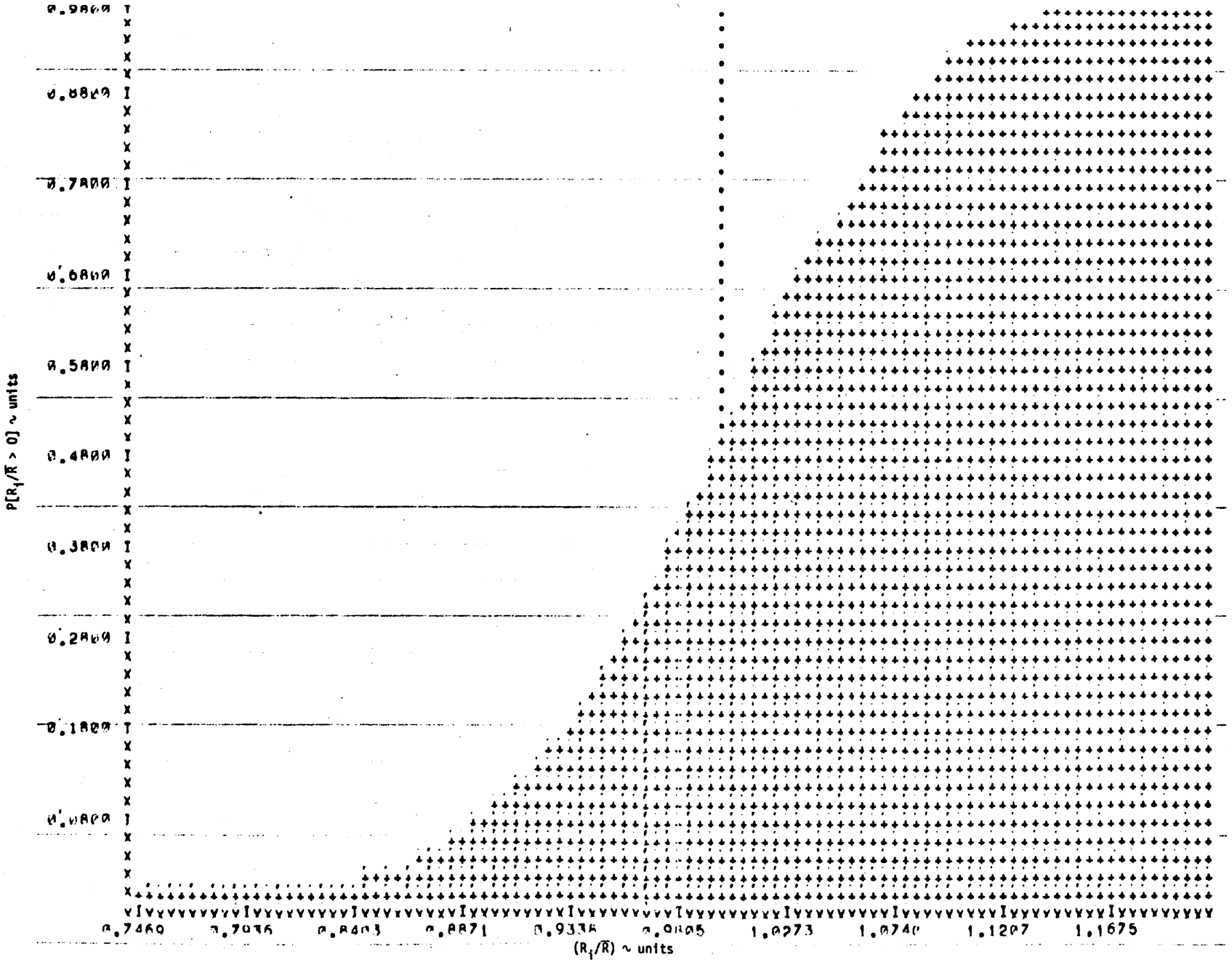

Figure 4. Cumulative Probability Distribution of $(R/\overline{R})$ for Variation of h.

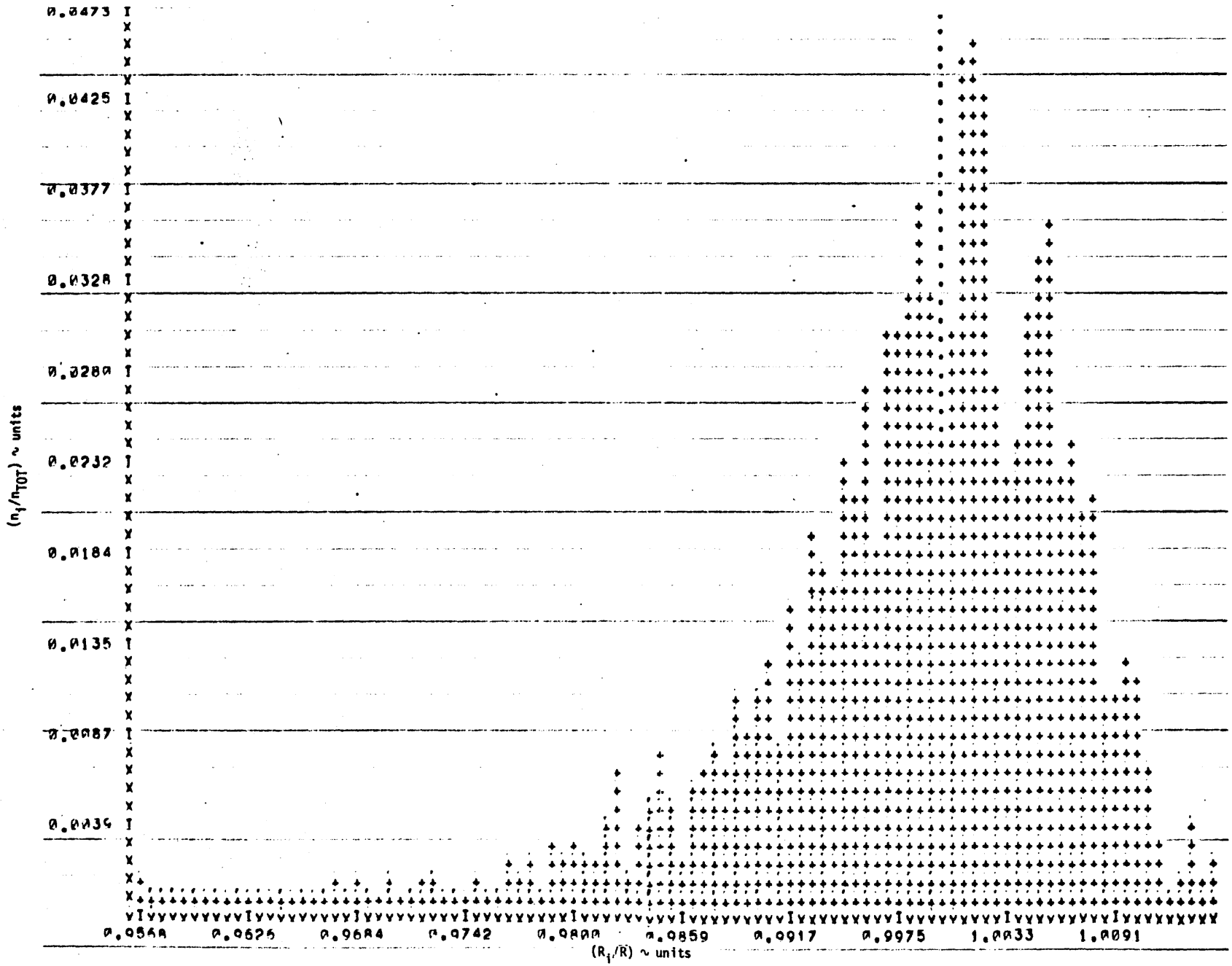

Figure 5. Probability Density of $(R/\overline{R})$ for Variation of ρ_p.

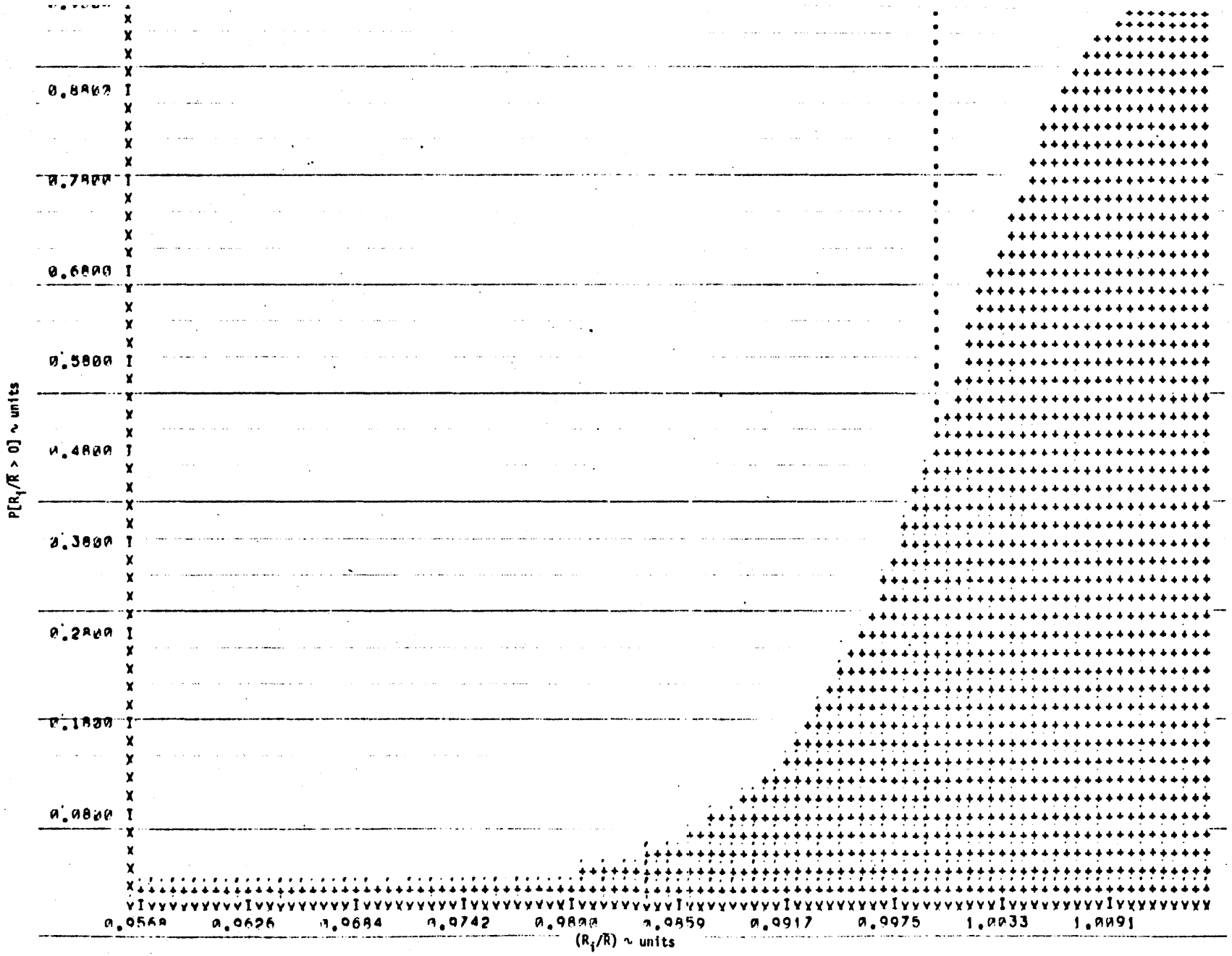

Figure 6. Cumulative Probability Distribution of $(R/\overline{R})$ for Variation of ρ_p.

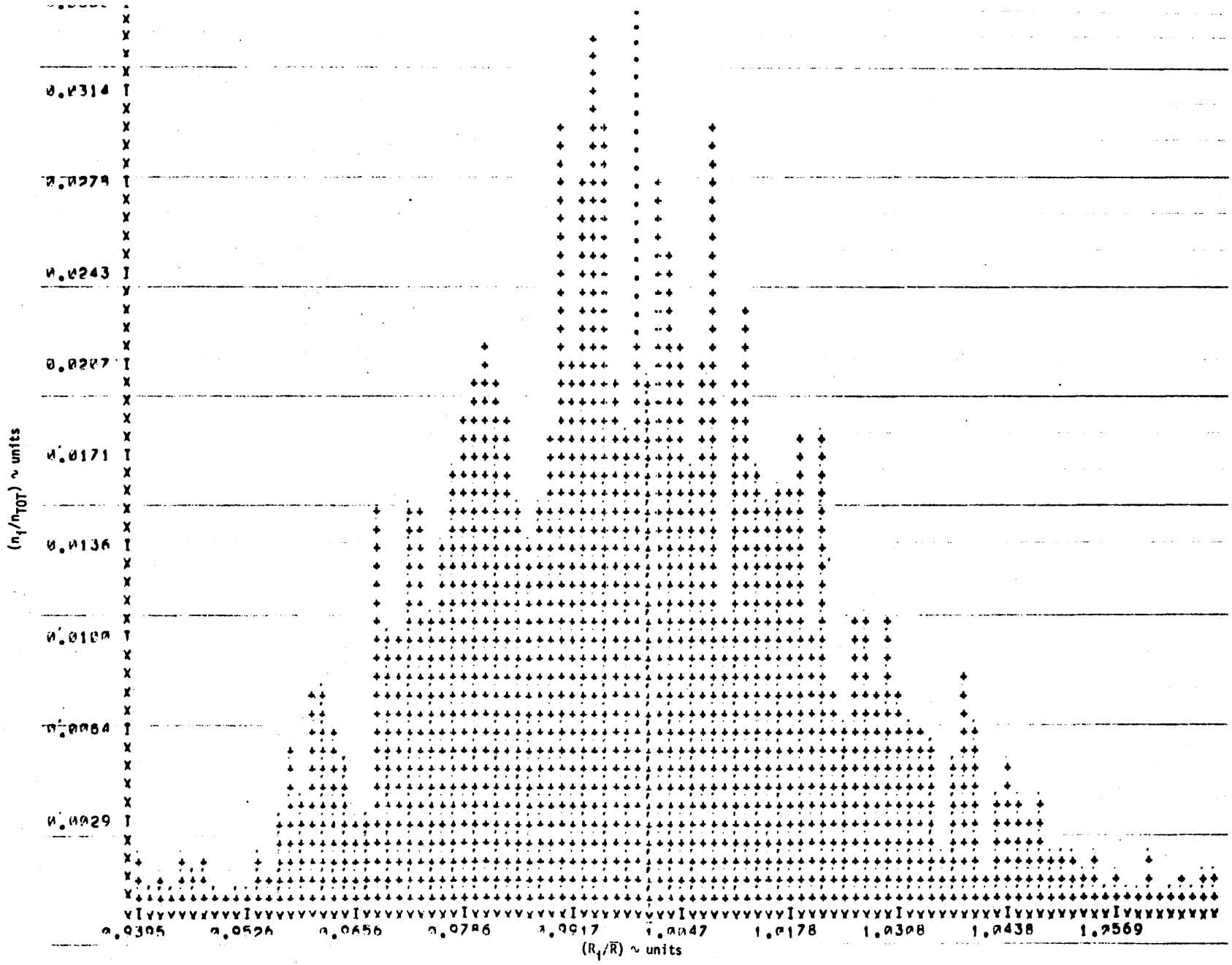

Figure 7. Probability Density of $(R/\overline{R})$ for Variation of S_T.

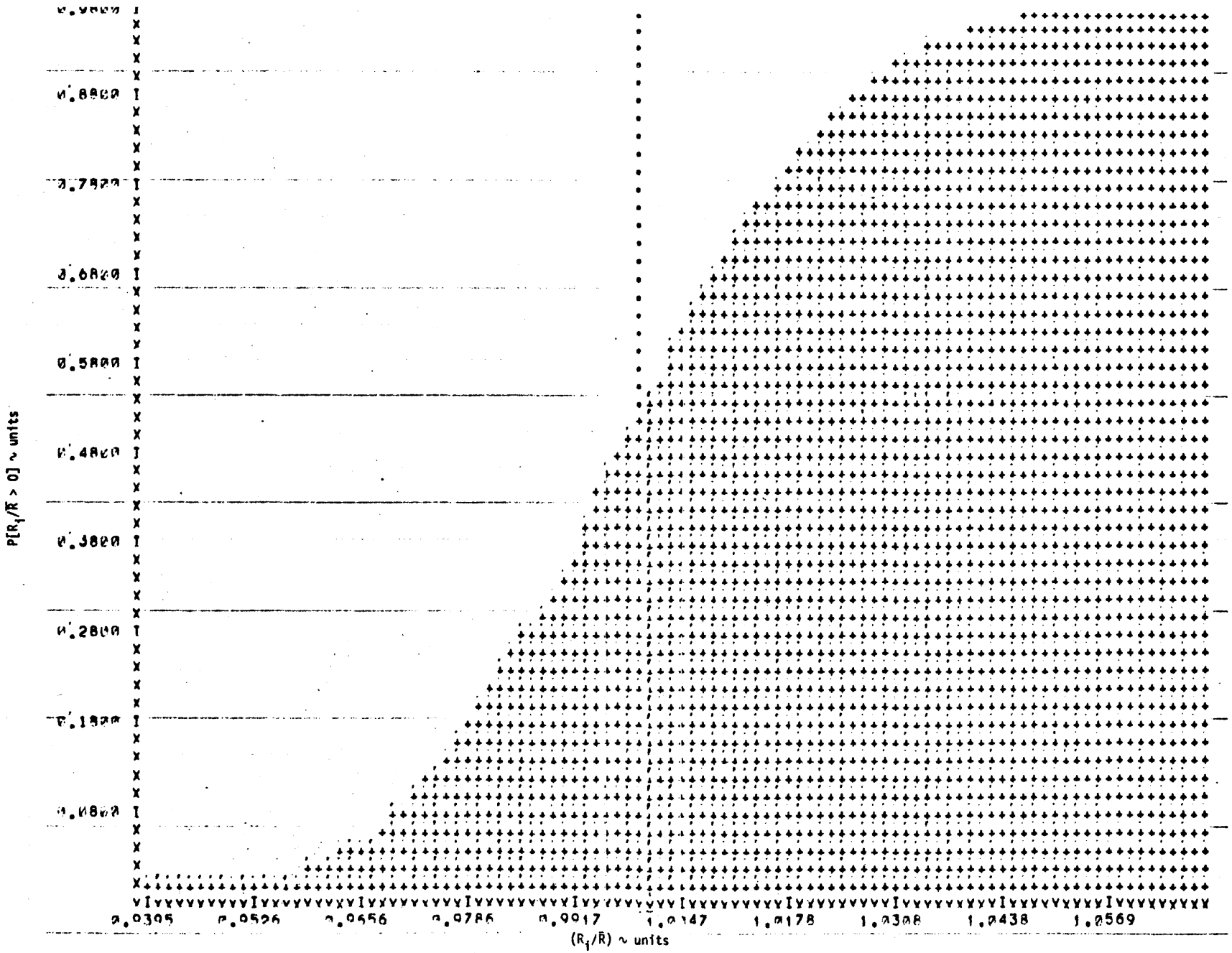

Figure 8. Cumulative Probability Distribution of $(R/\overline{R})$ for Variation of S_T.

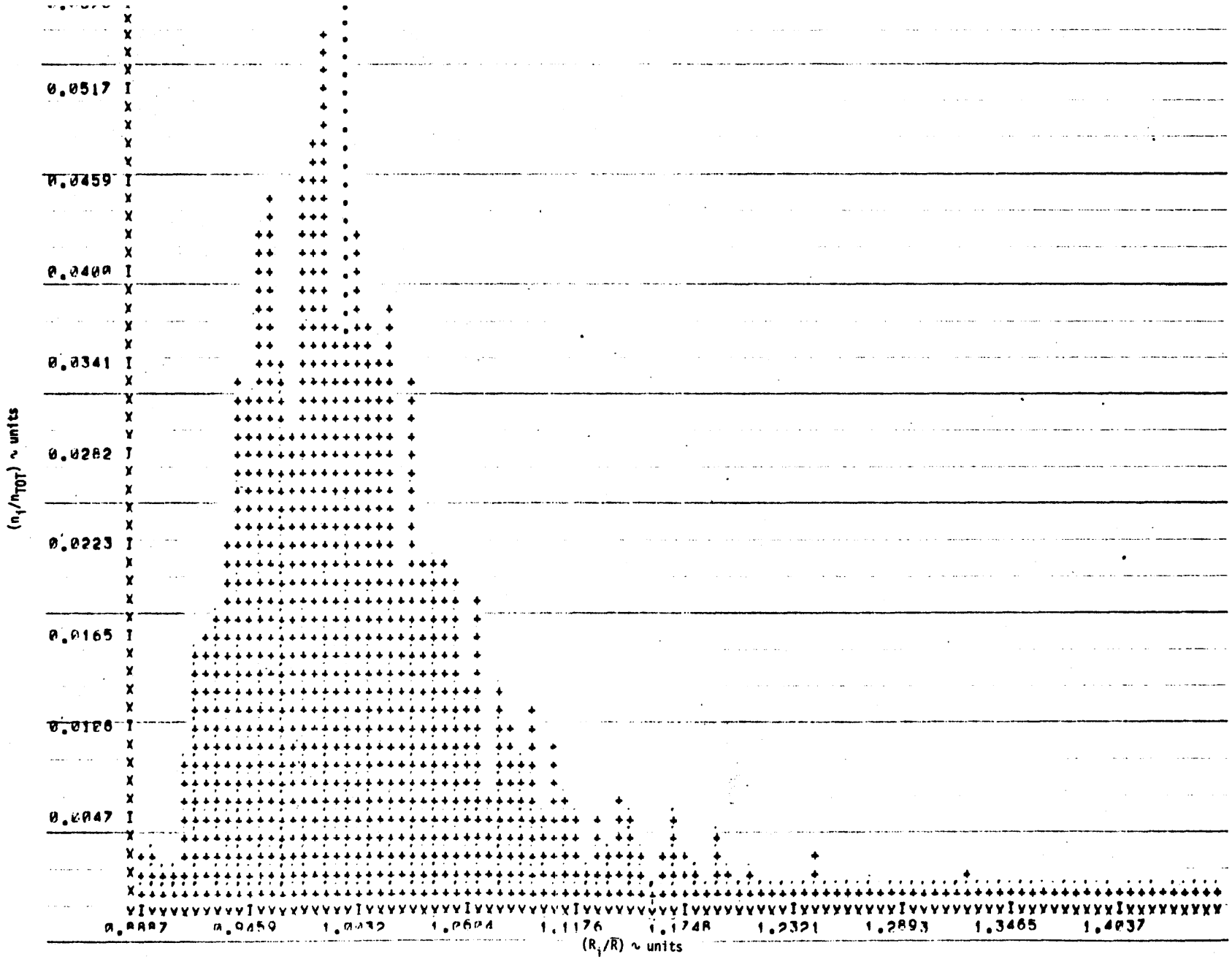

Figure 9. Probability Density of $(R/\overline{R})$ for Variation of S_E.

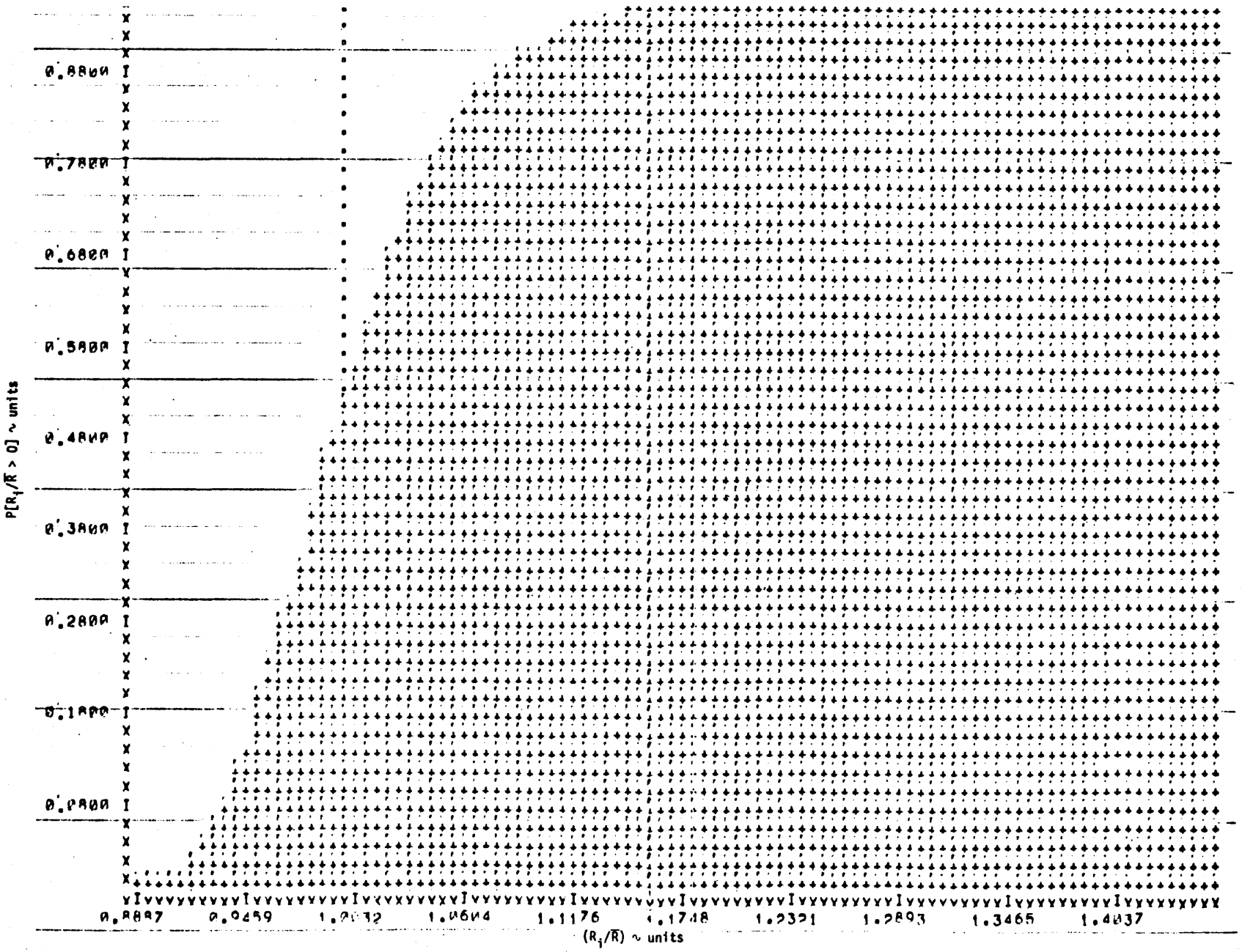

Figure 10. Cumulative Probability Distribution of $(R/\overline{R})$ for Variation of S_E.

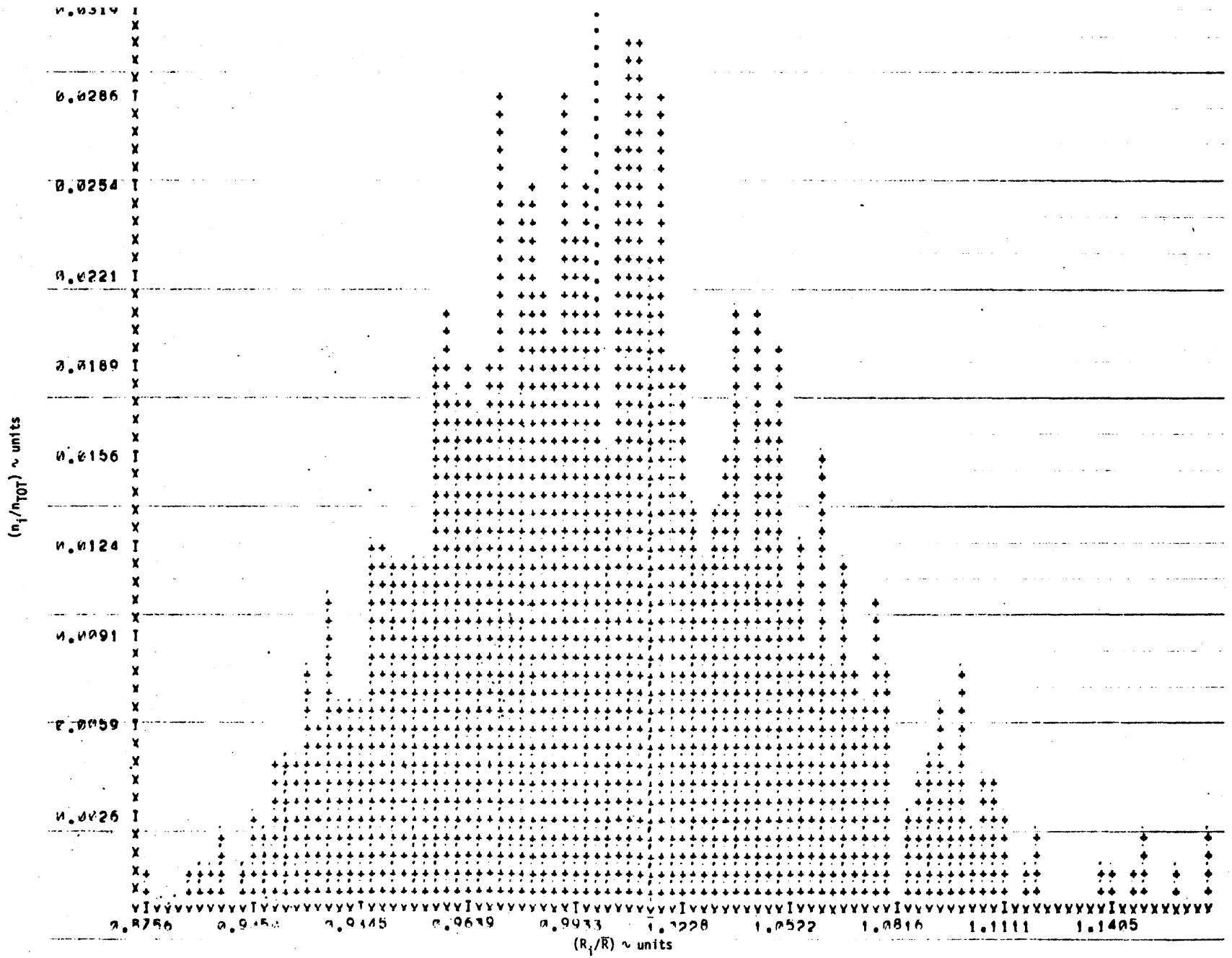

Figure 11. Probability Density of $(R/\bar{R})$ for Variation of $\tan\phi$.

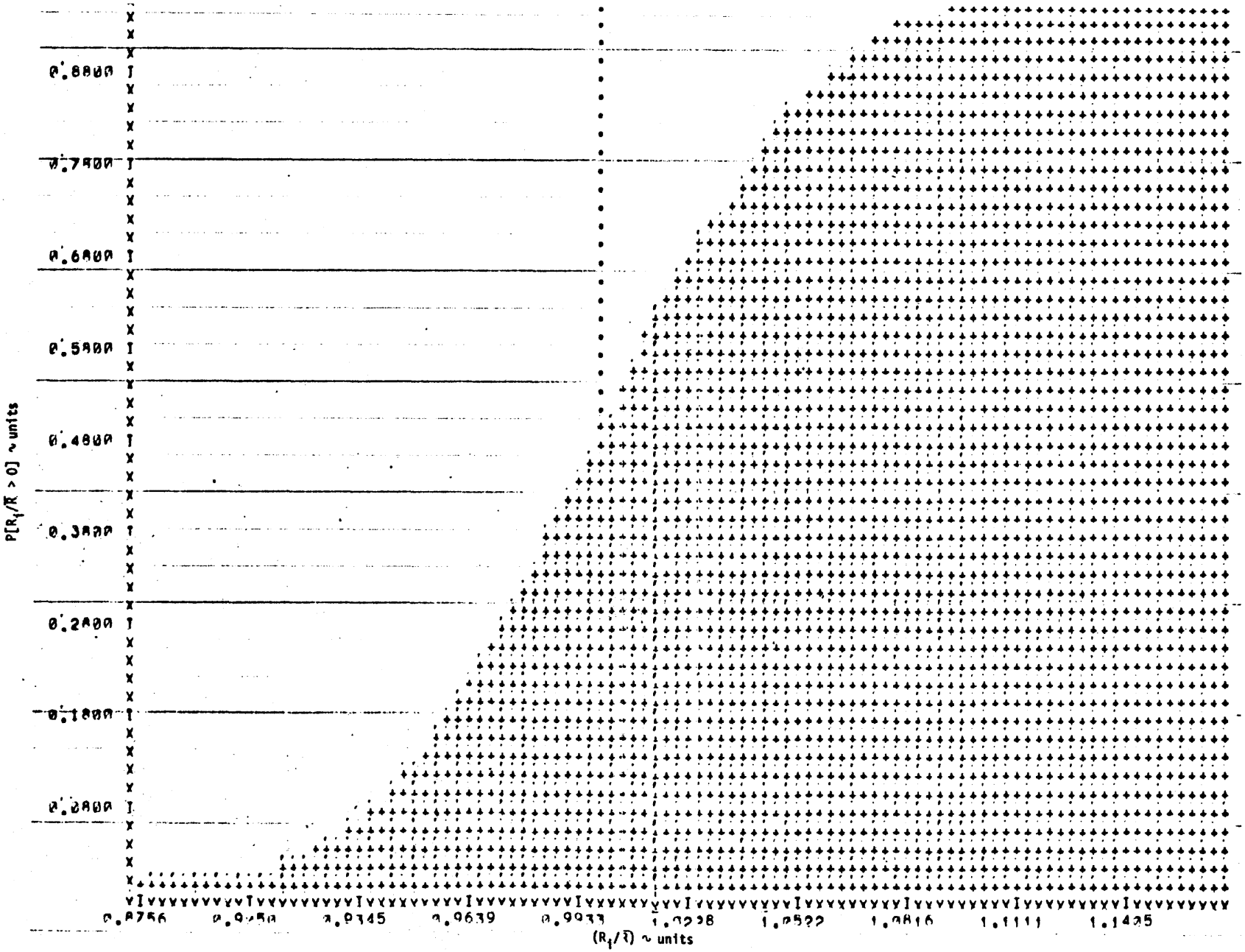

Figure 12. Cumulative Probability Distribution of $(R/\overline{R})$ for Variation of $\tan\phi$.

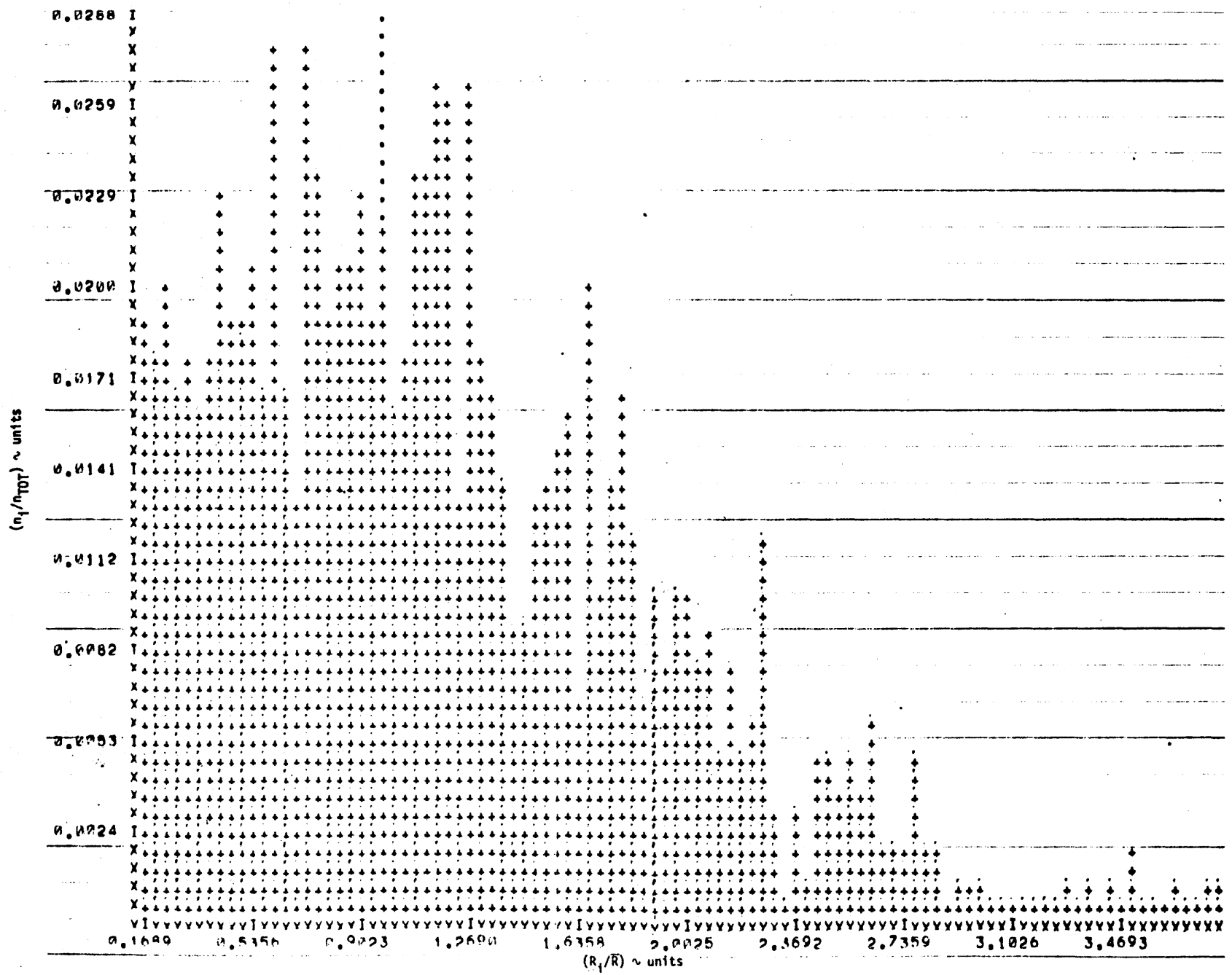

Figure 13. Probability Density of $(R/\overline{R})$ for Variation of u.

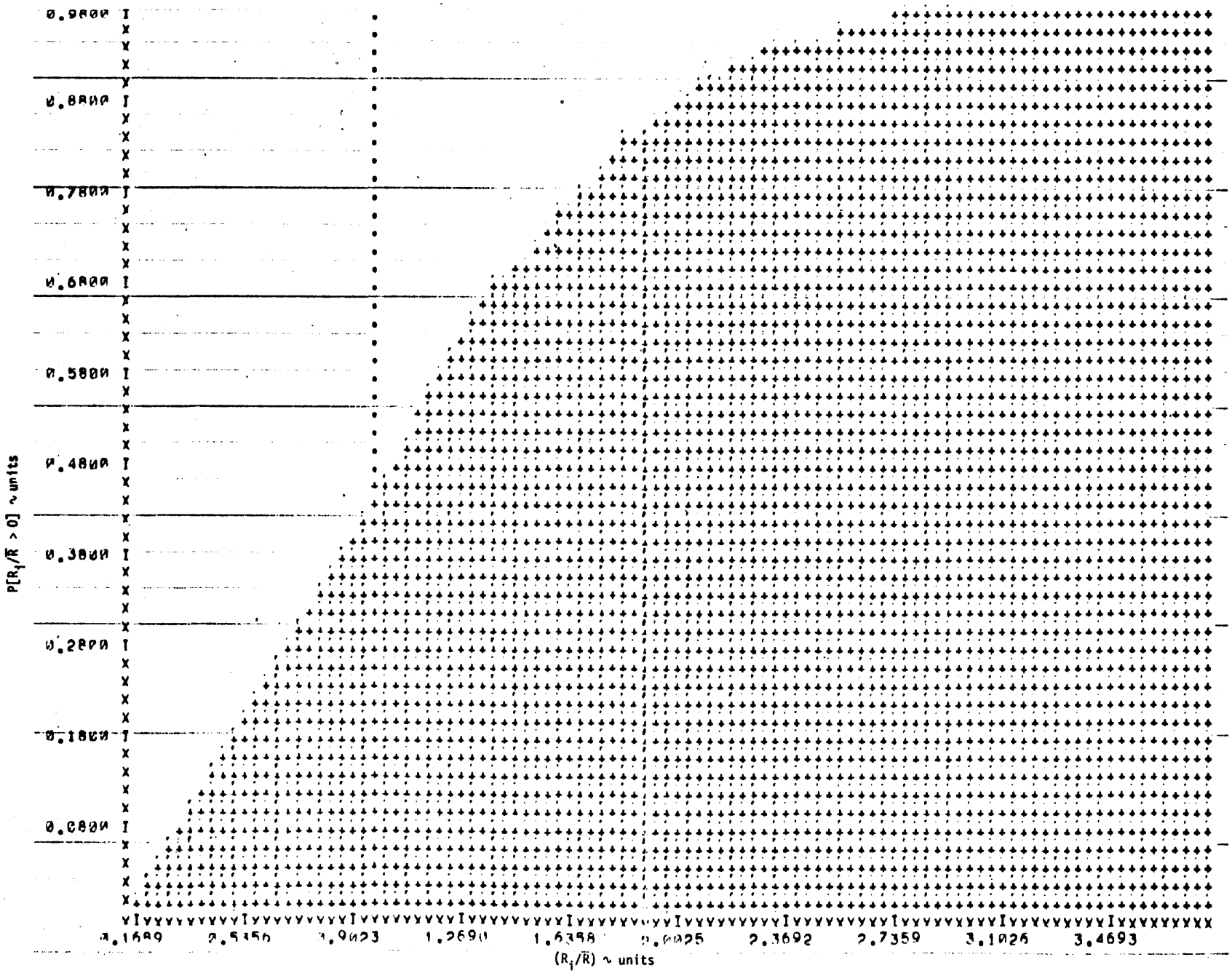

Figure 14. Cumulative Probability Distribution of $(R/\bar{R})$ for Variation of u.

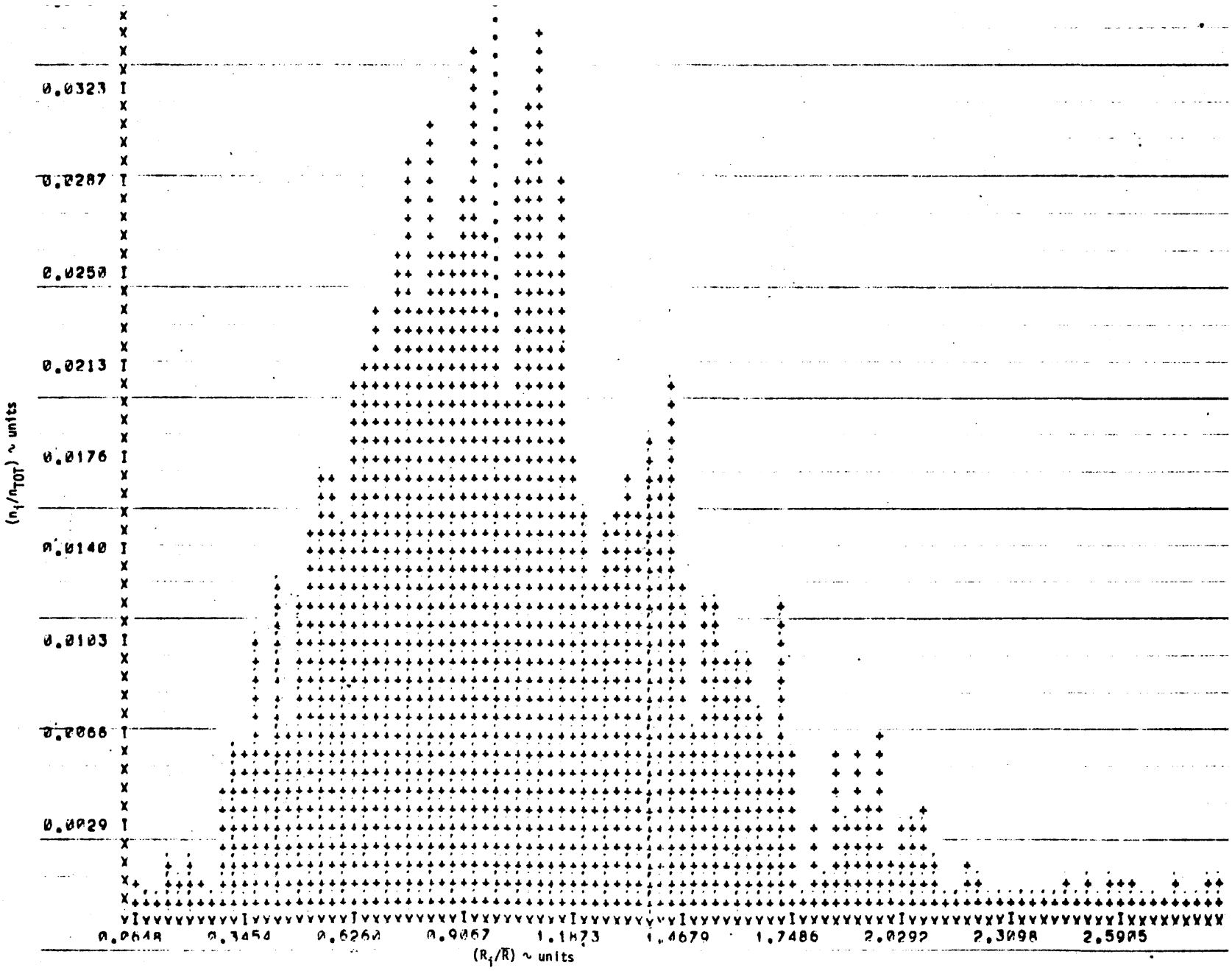

Figure 15. Probability Density of $(R/\overline{R})$ for Variation of σ.

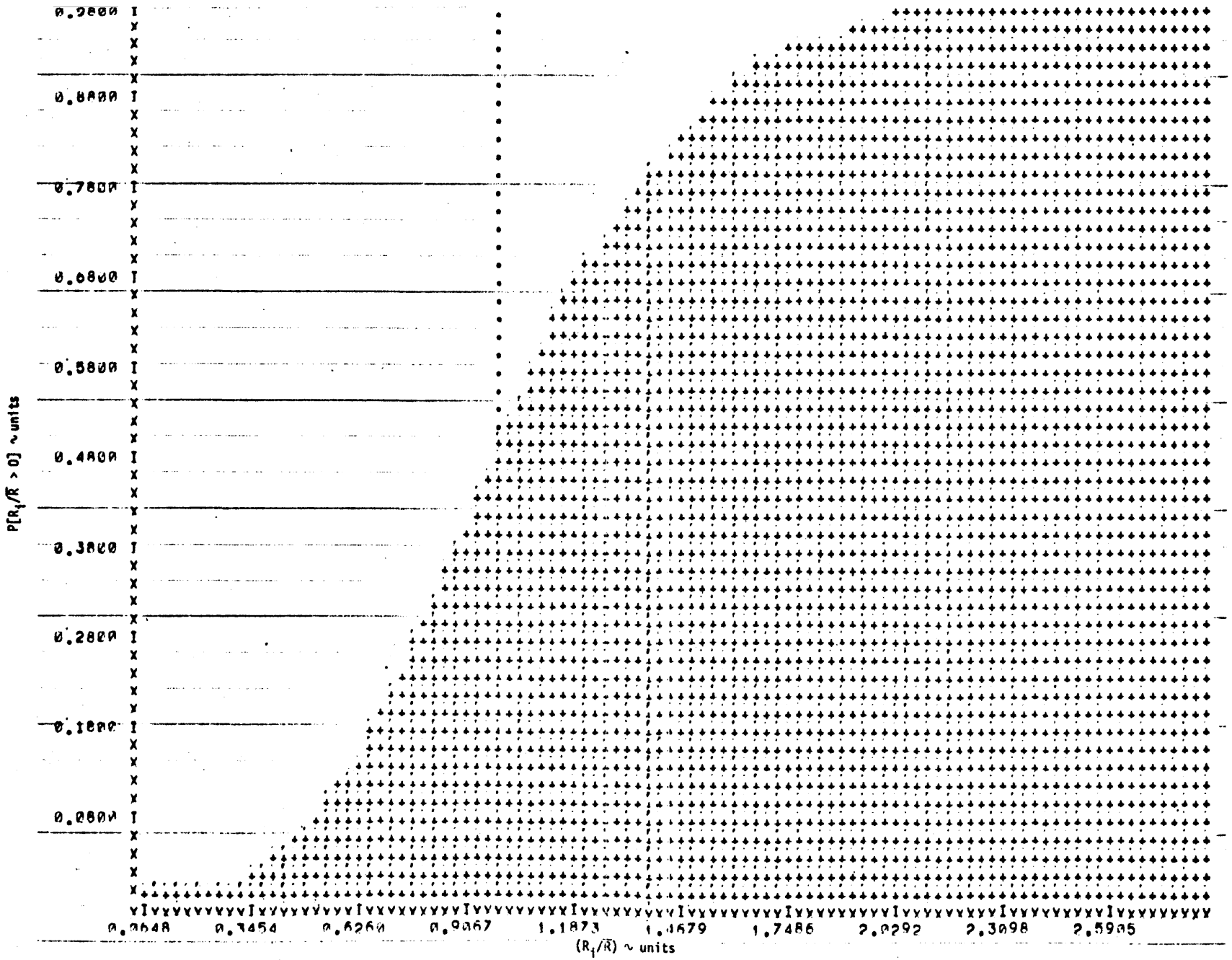

Figure 16. Cumulative Probability Distribution of $(R/\bar{R})$ for Variation of σ.

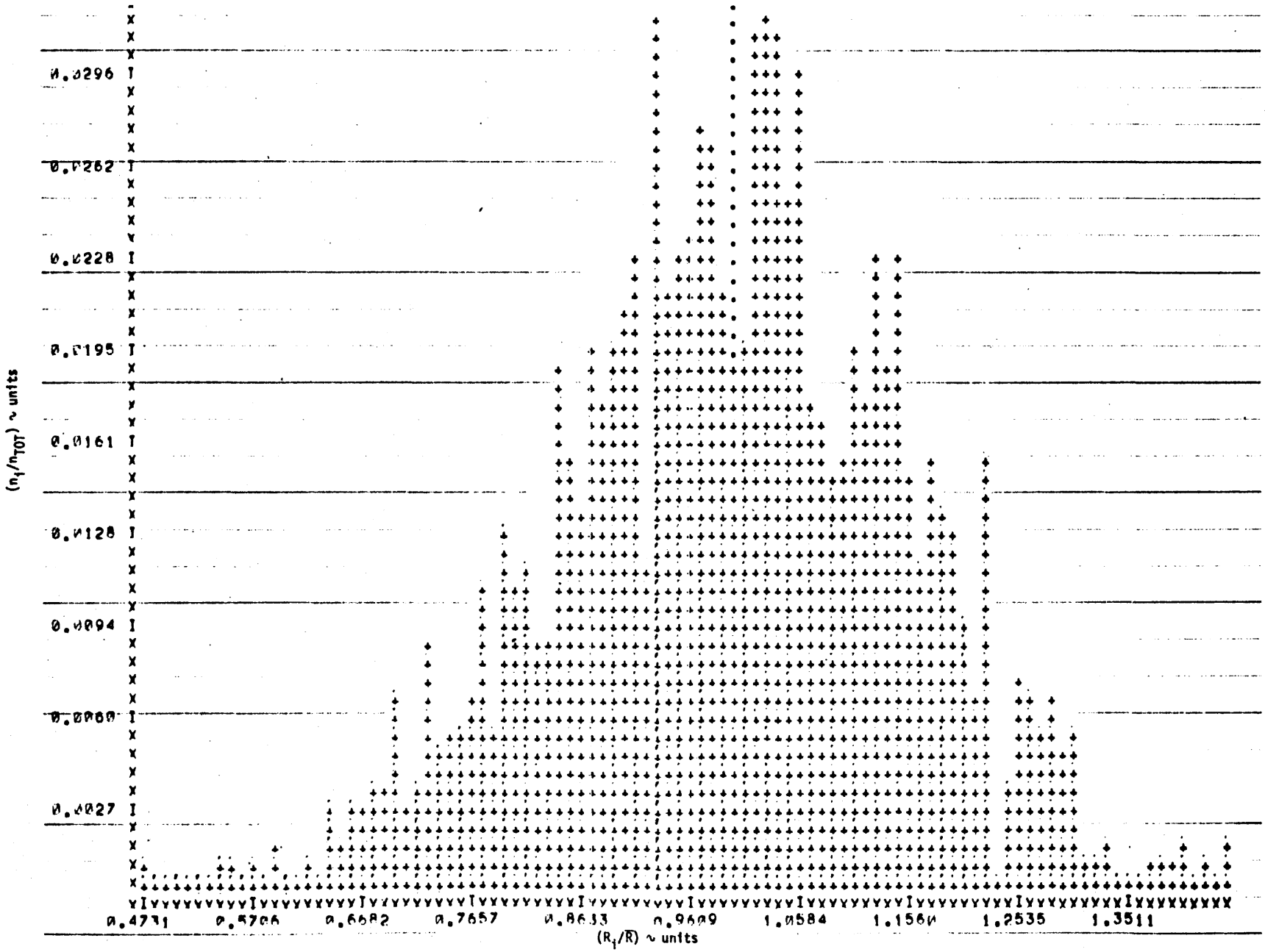

Figure 17 Probability Density of $(R/\bar{R})$ for Variation of δ

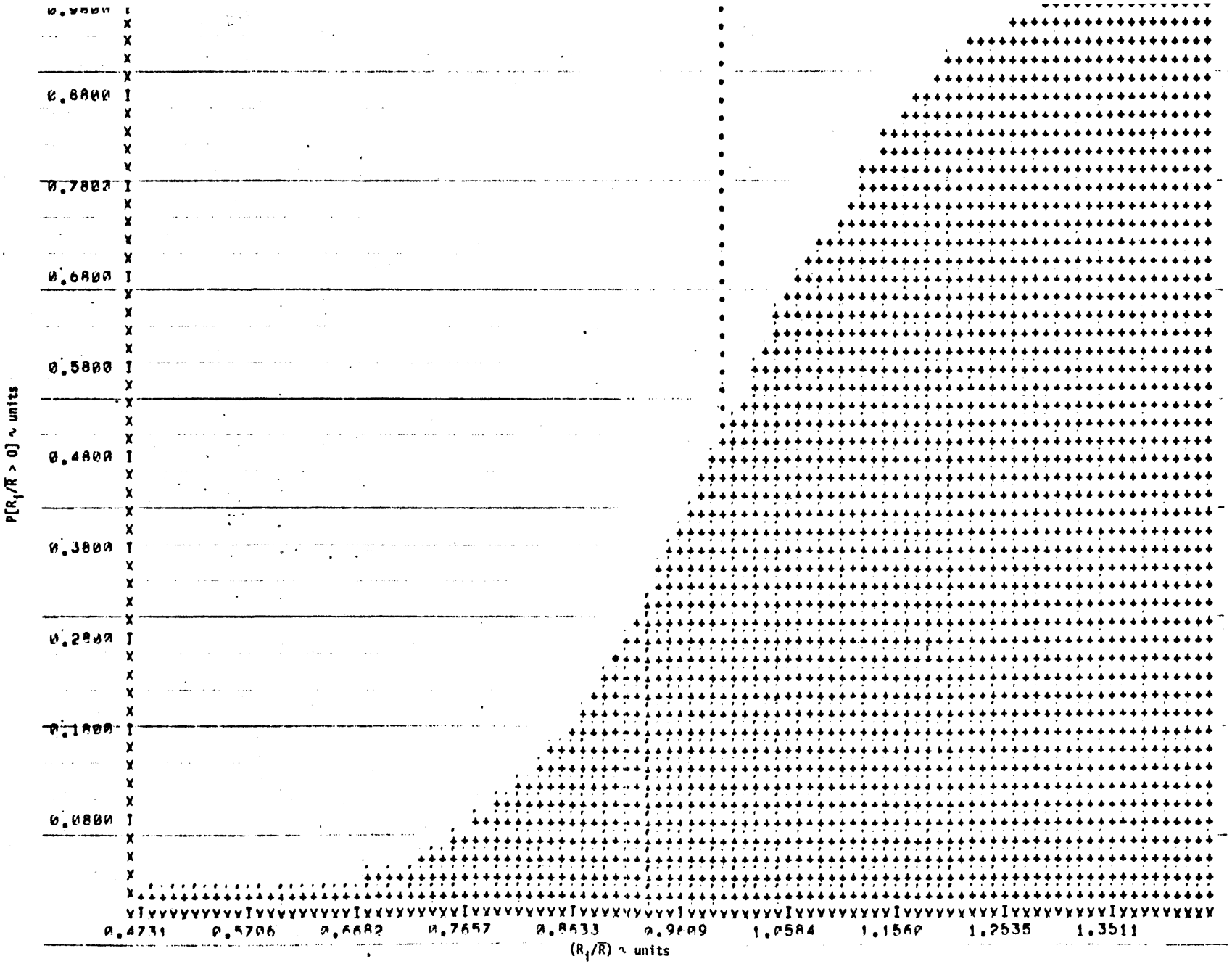

Figure 18. Cumulative Probability Distribution of $(R/\bar{R})$ for Variation of δ.

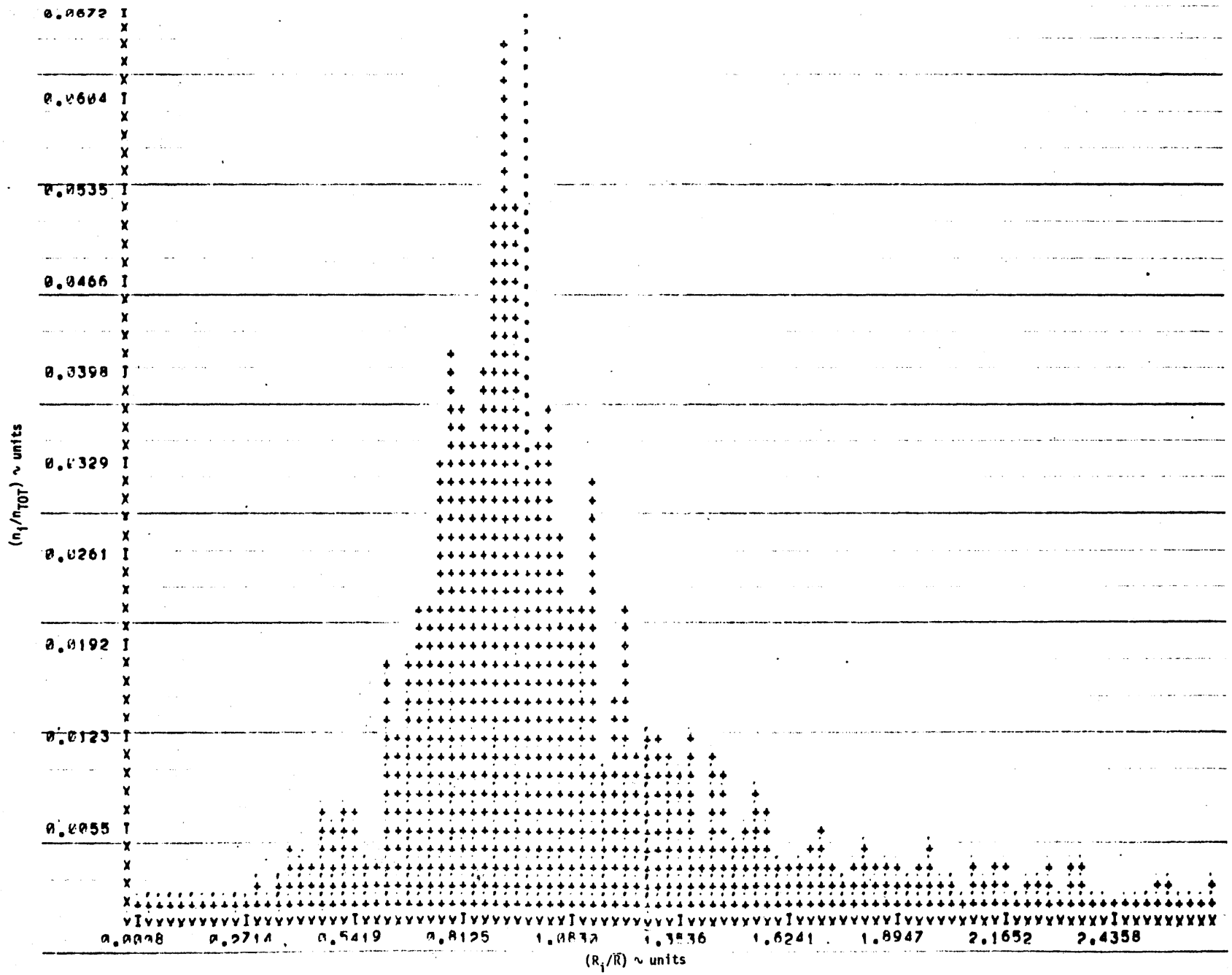

Figure 19. Probability Density of $(R/\overline{R})$ for Variation of M_f.

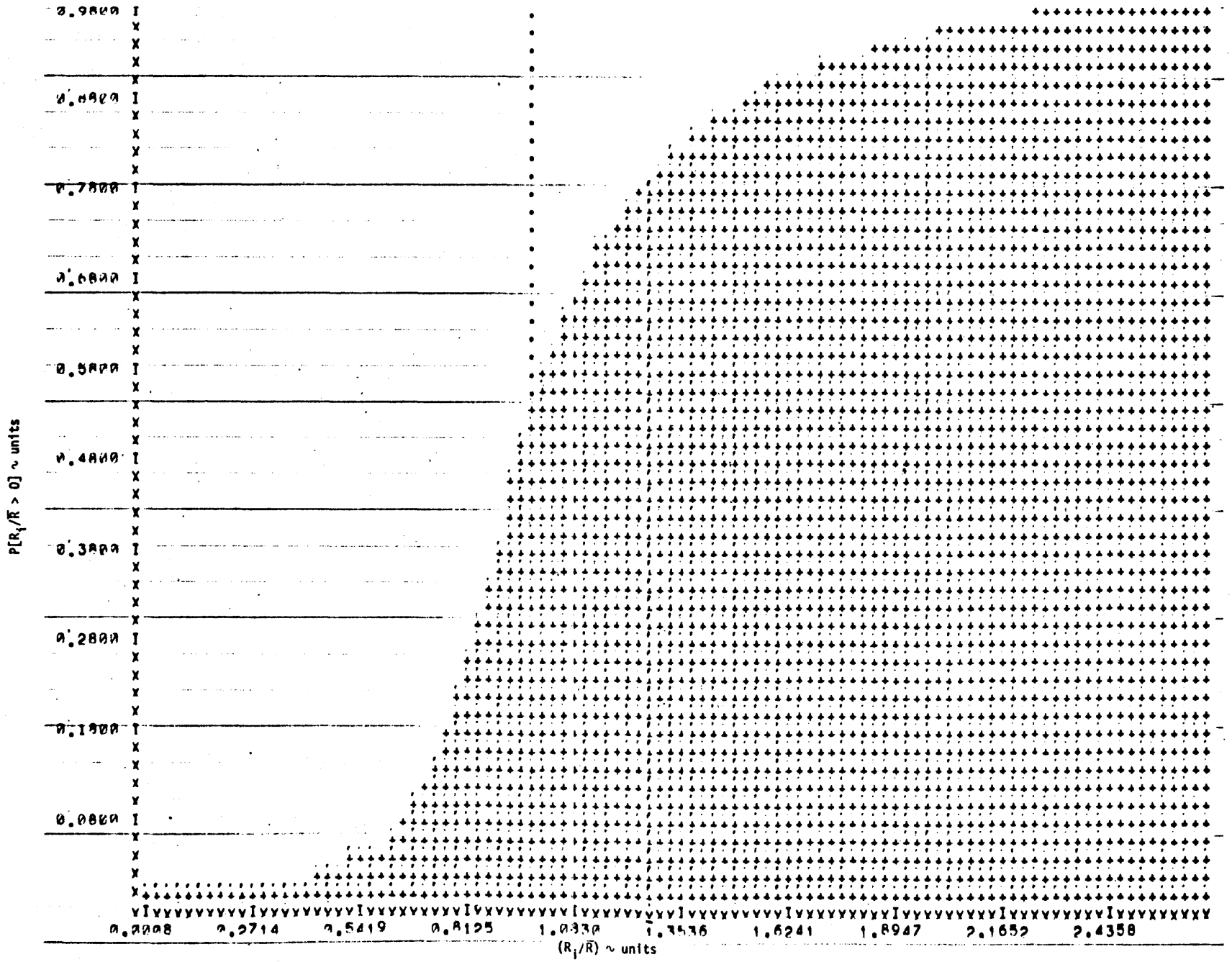

Figure 20. Cumulative Probability Distribution of $(R/\overline{R})$ for Variation of M_f.

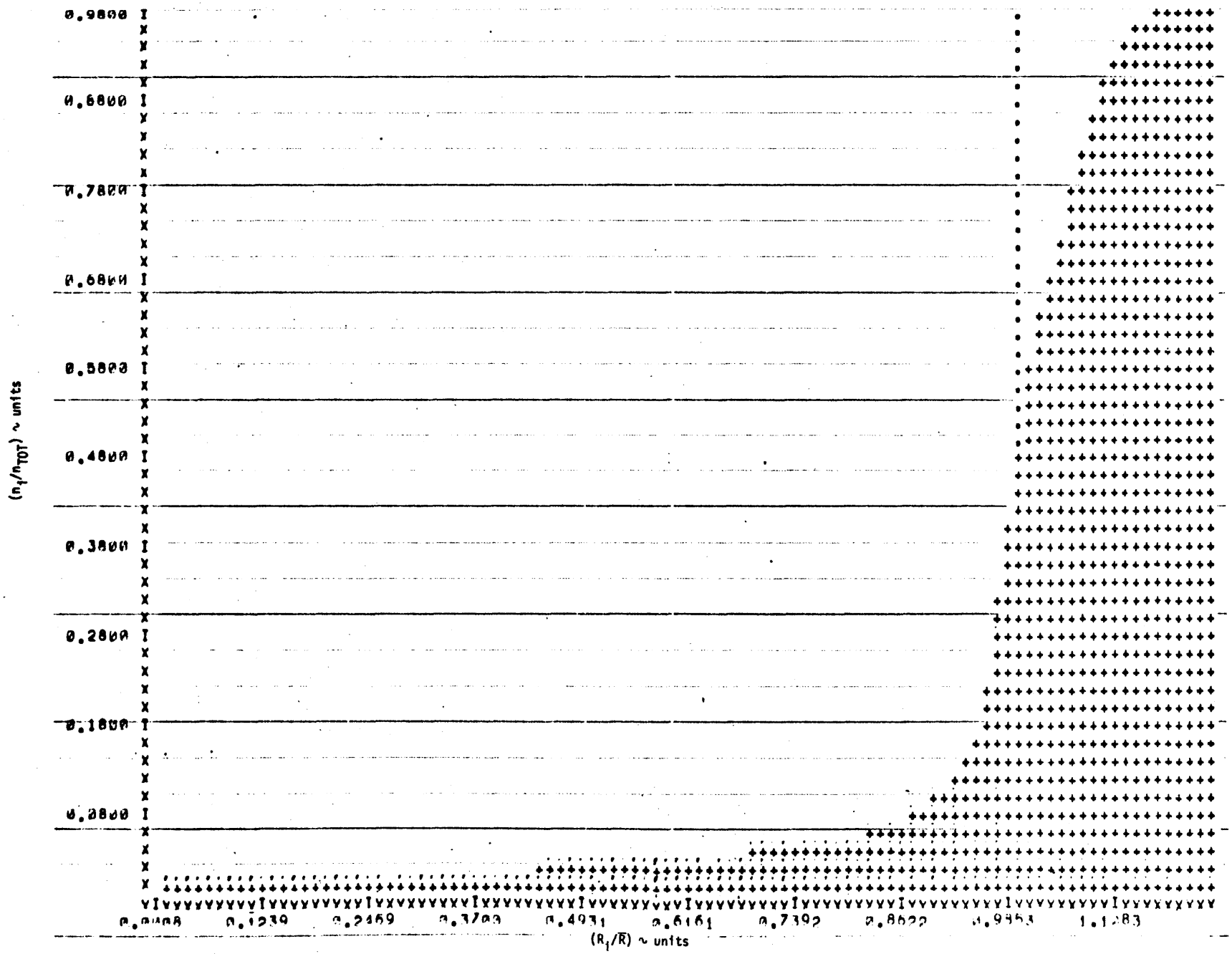

Figure 21. Probability Density of $(R/\overline{R})$ for Variation of M_x.

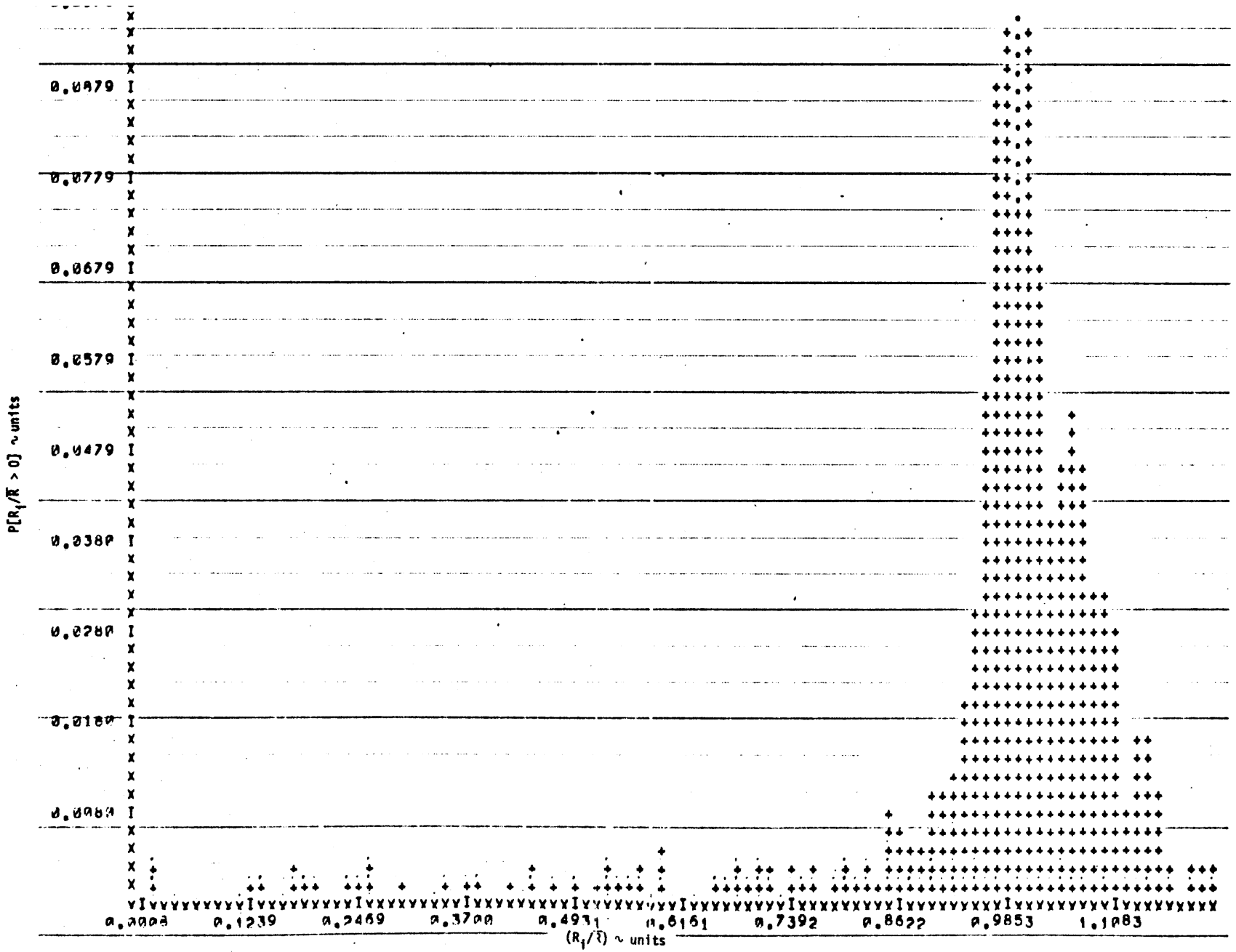

Figure 22. Cumulative Probability Distribution of $(R/\overline{R})$ for Variation of M_x.

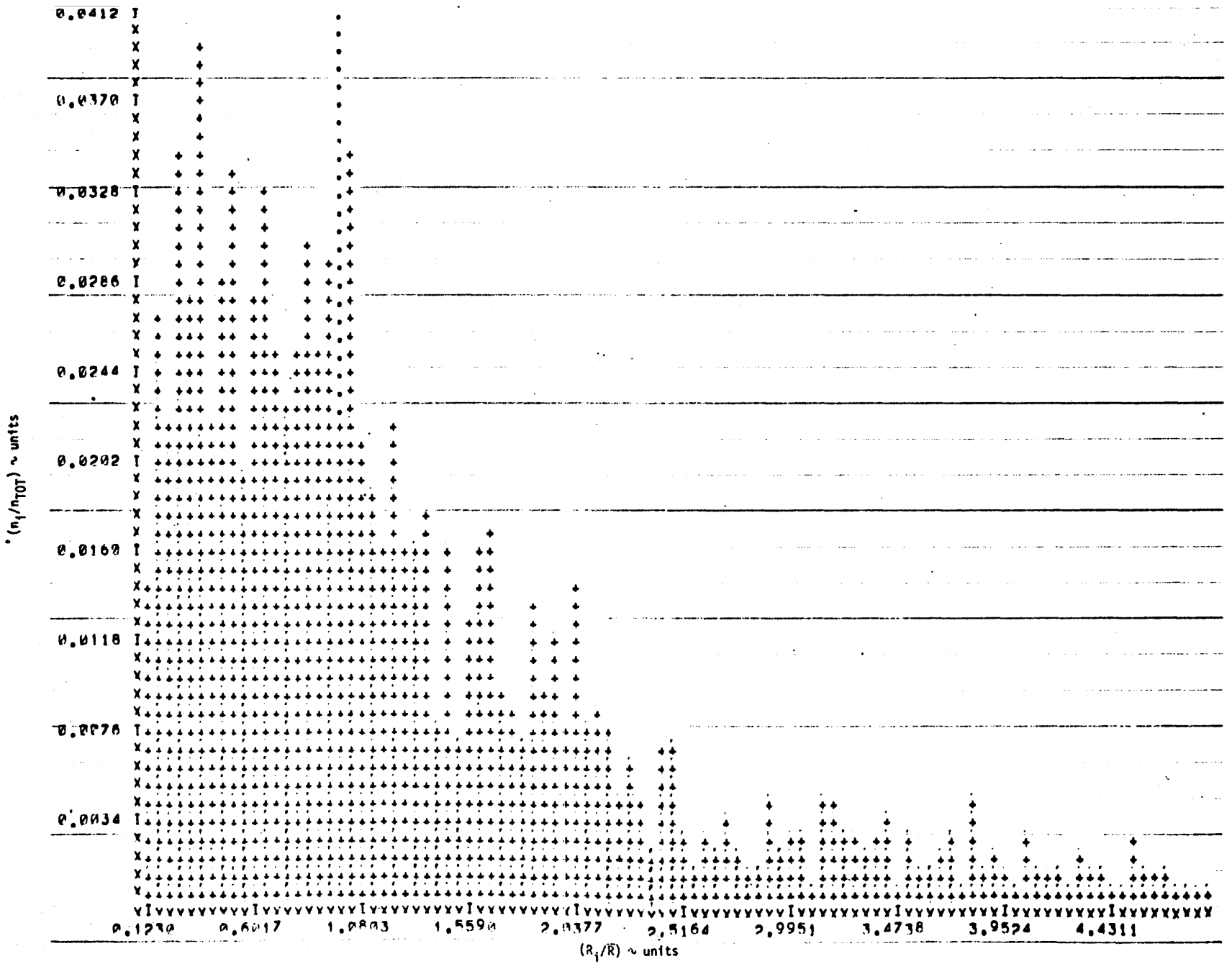

Figure 23. Probability Density of $(R/\overline{R})$ for Variation of u,σ.

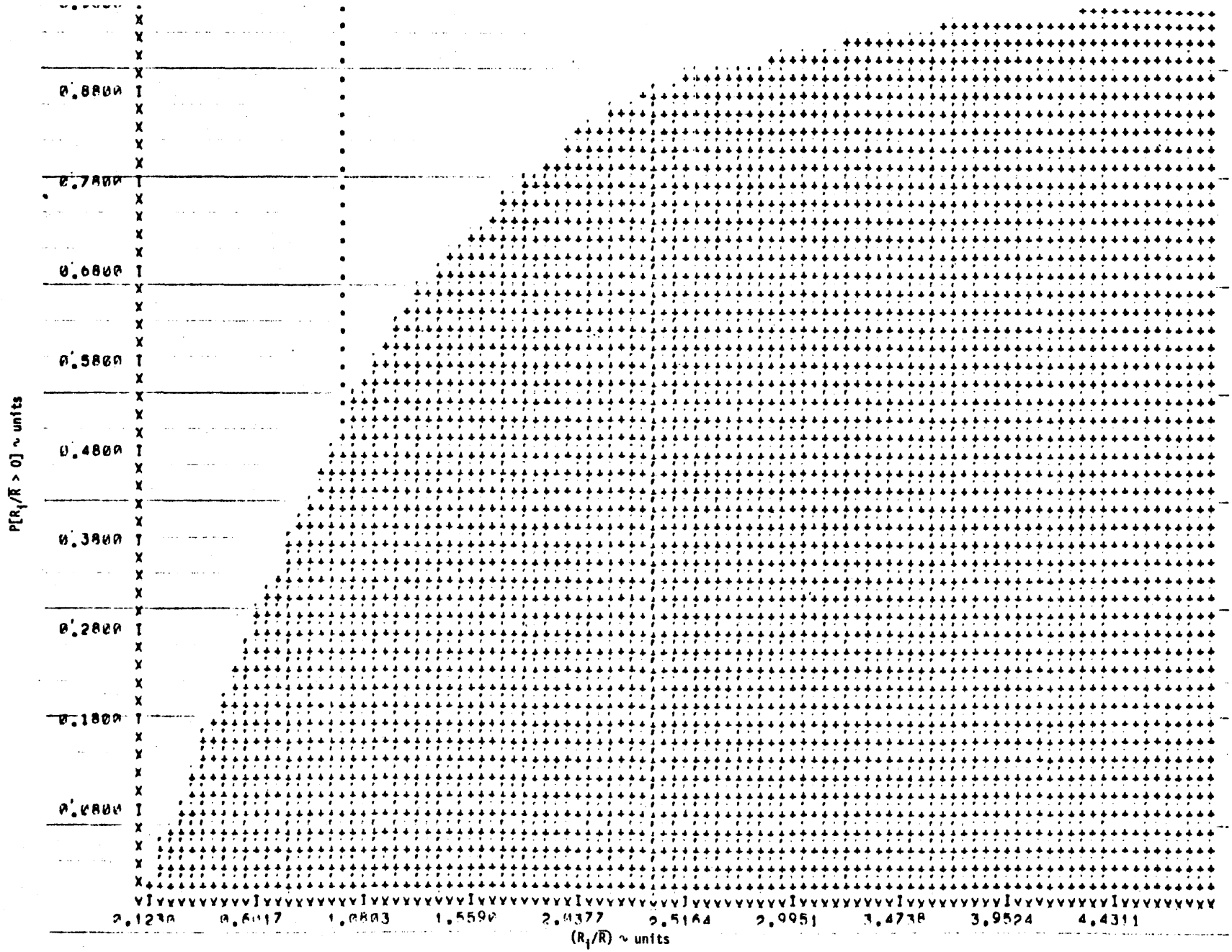

Figure 24. Cumulative Probability Distribution of $(R/\overline{R})$ for Variation of u,σ.

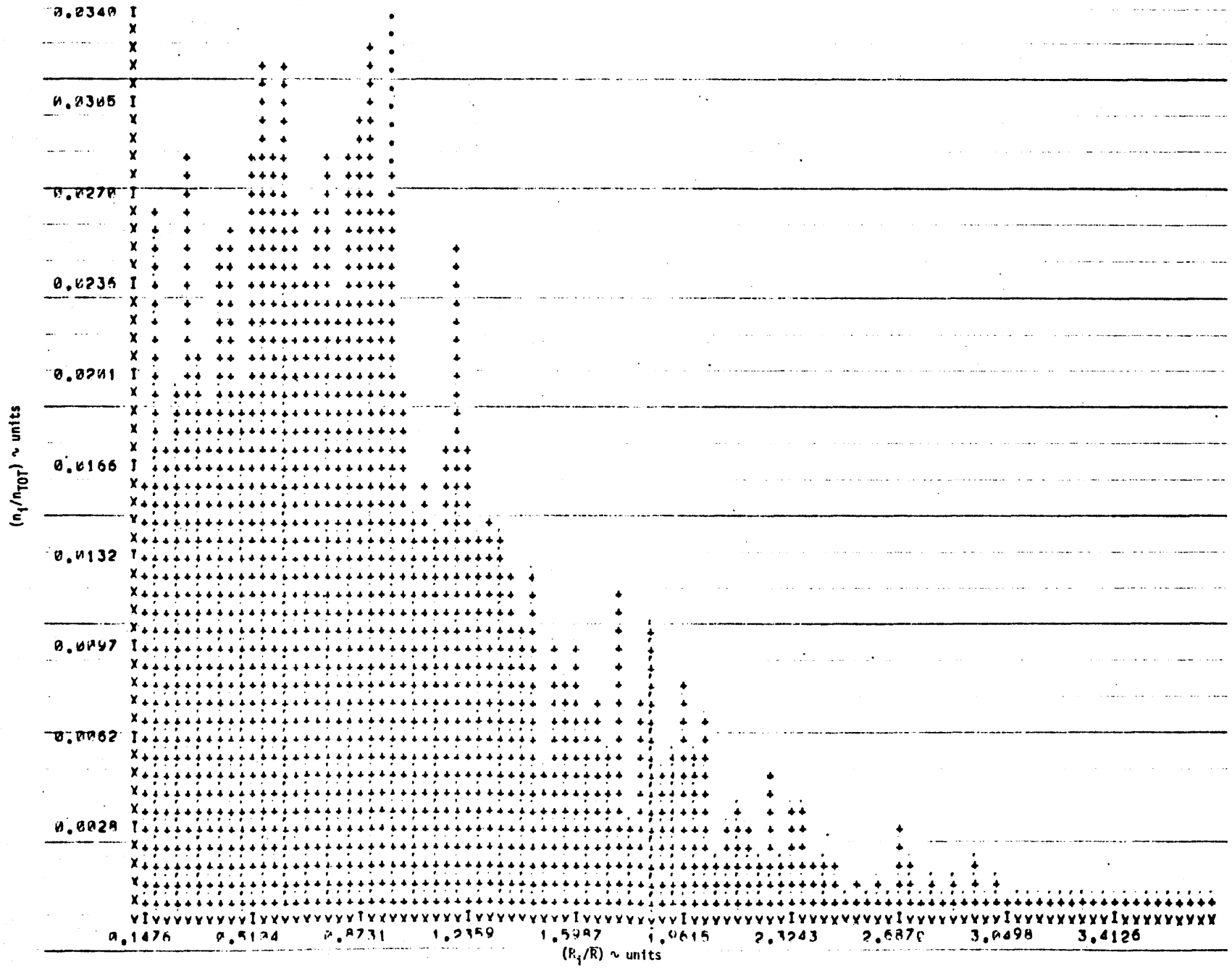

Figure 25. Probability Density of $(R/\bar{R})$ for Variation of u,δ.

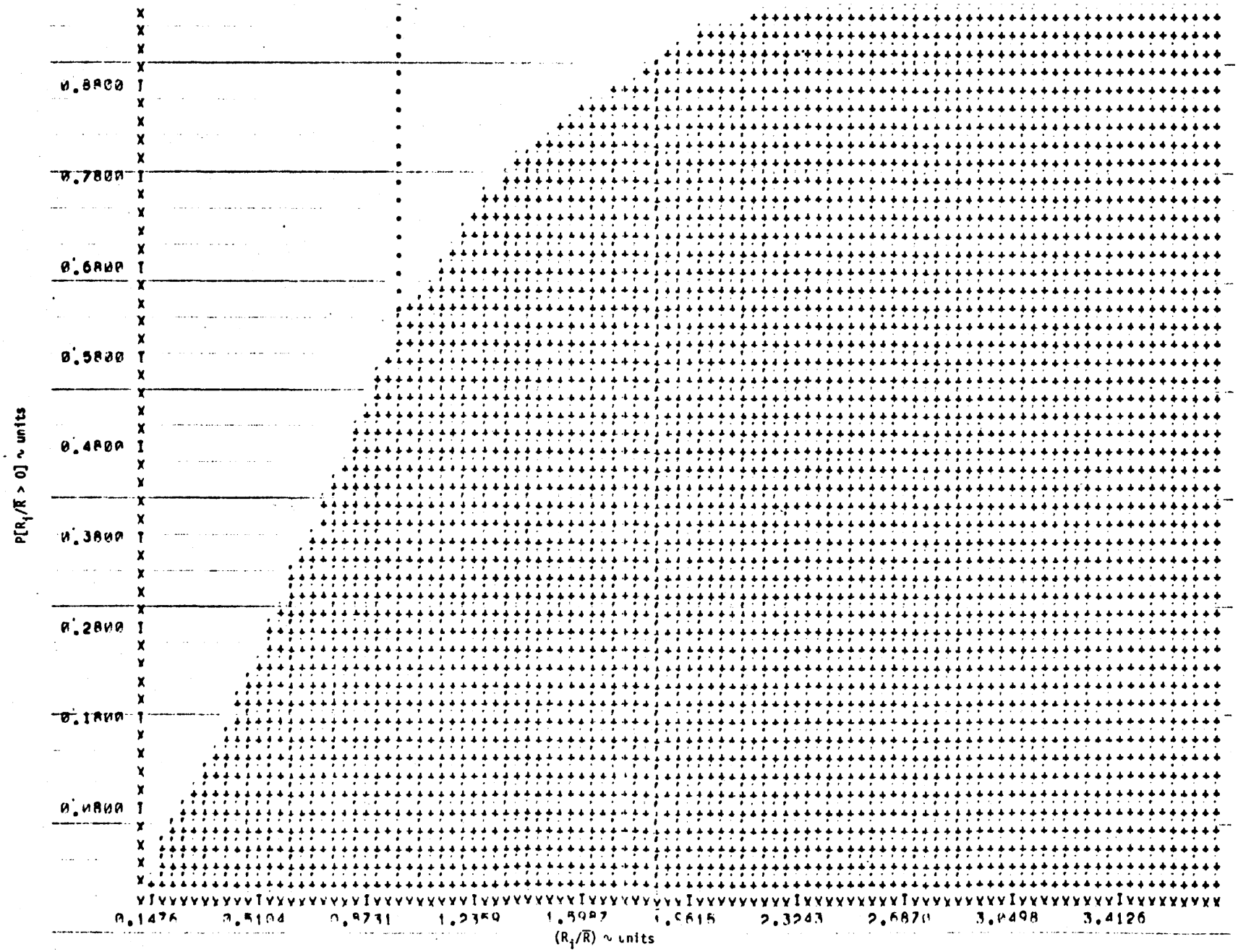

Figure 26. Cumulative Probability Distribution of $(R/\bar{R})$ for Variation of u,δ.

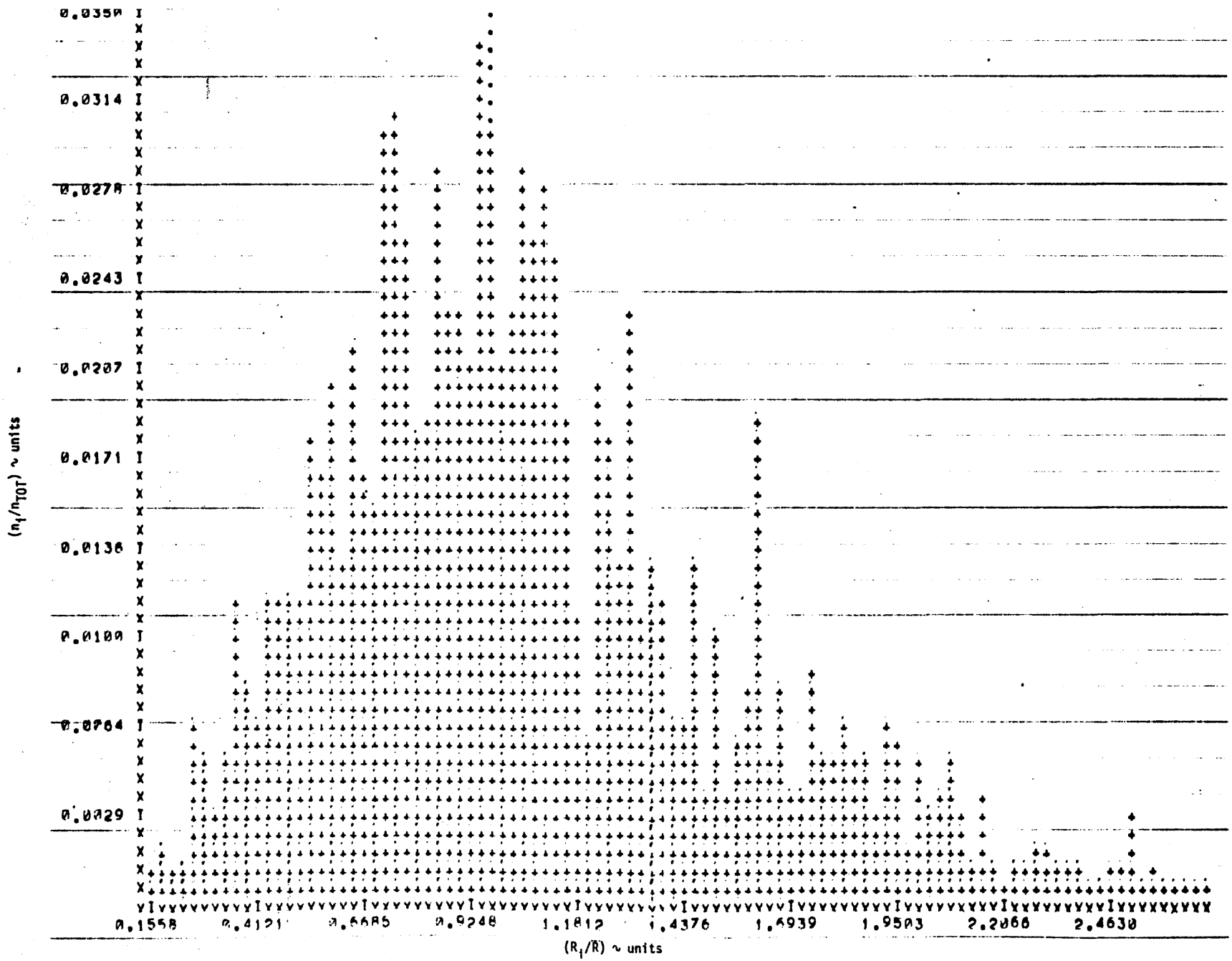

Figure 27. Probability Density of $(R/\bar{R})$ for Variation of σ,δ.

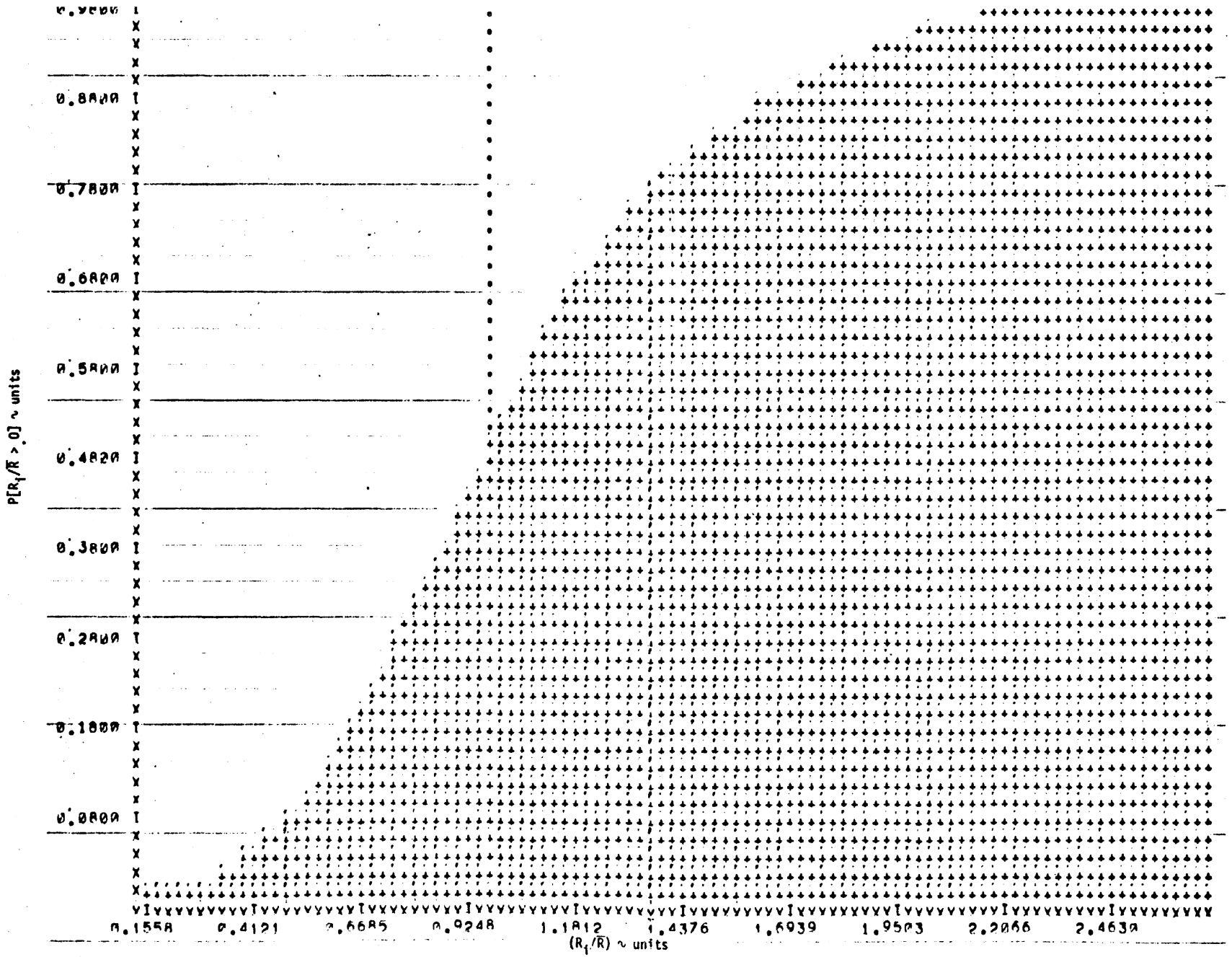

Figure 28. Cumulative Probability Distribution of $(R/\overline{R})$ for Variation of σ,δ.

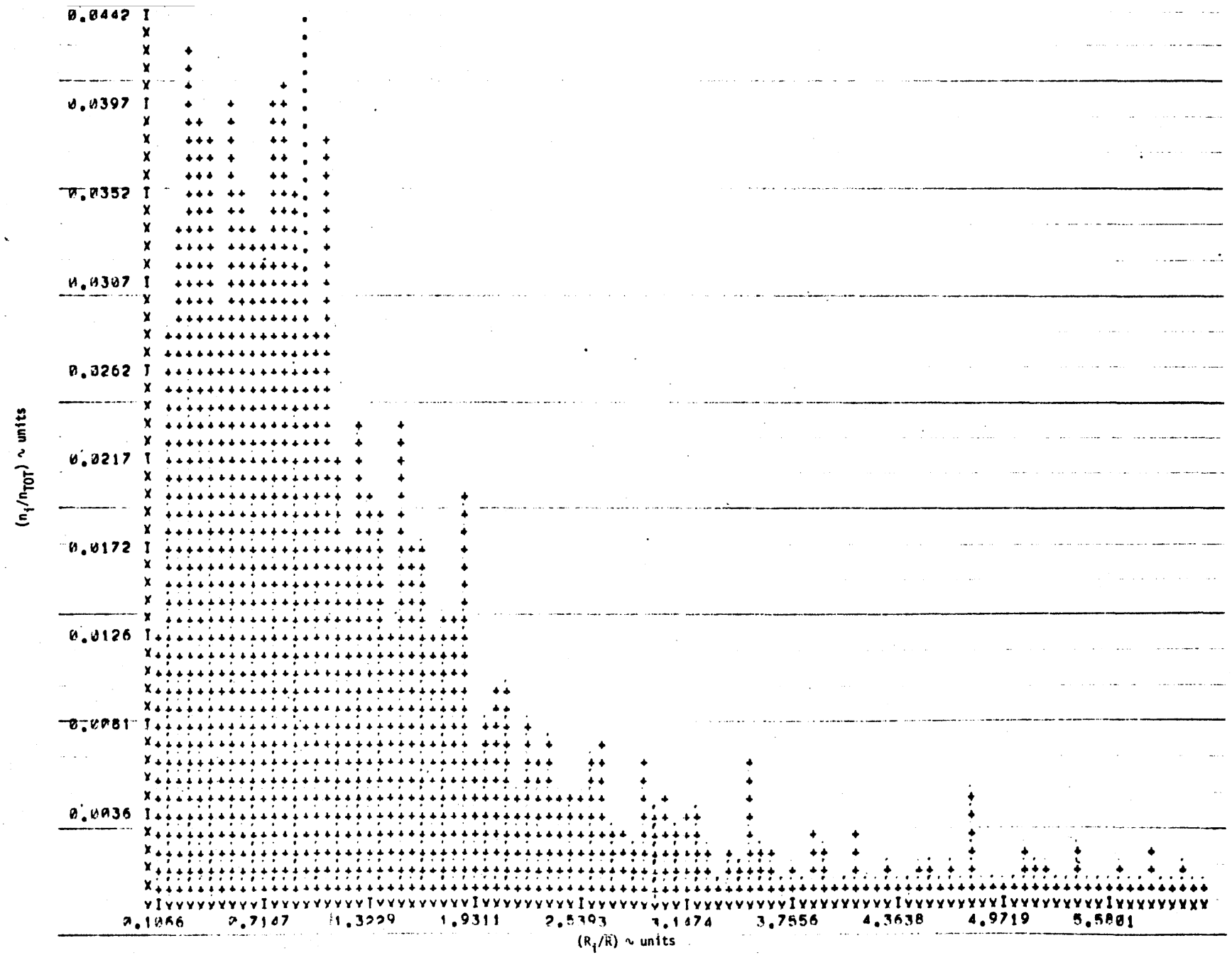

Figure 29. Probability Density of $(R/\bar{R})$ for Variation of u,σ,δ.

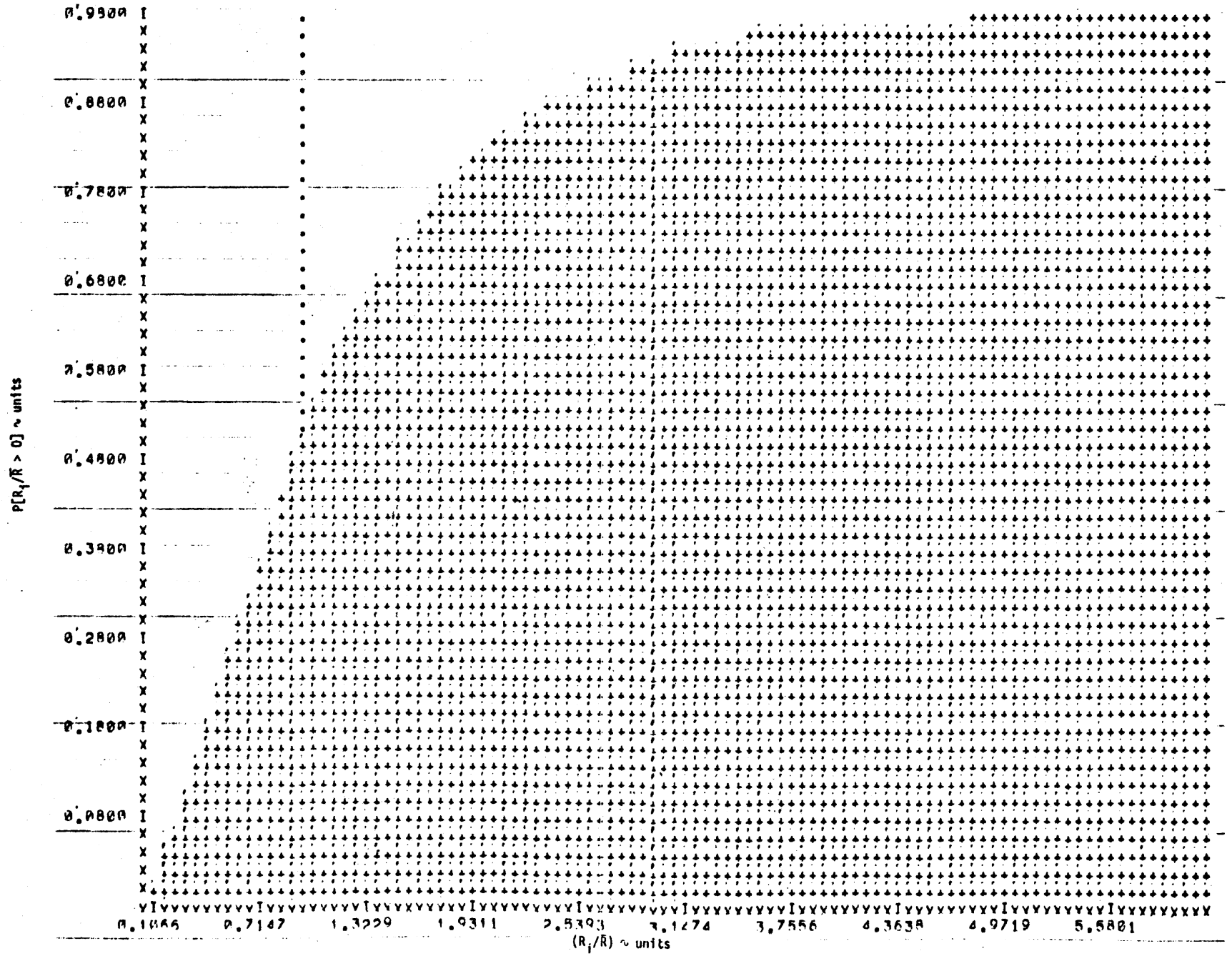

Figure 30. Cumulative Probability Distribution of $(R/\overline{R})$ for Variation of u,σ,δ.

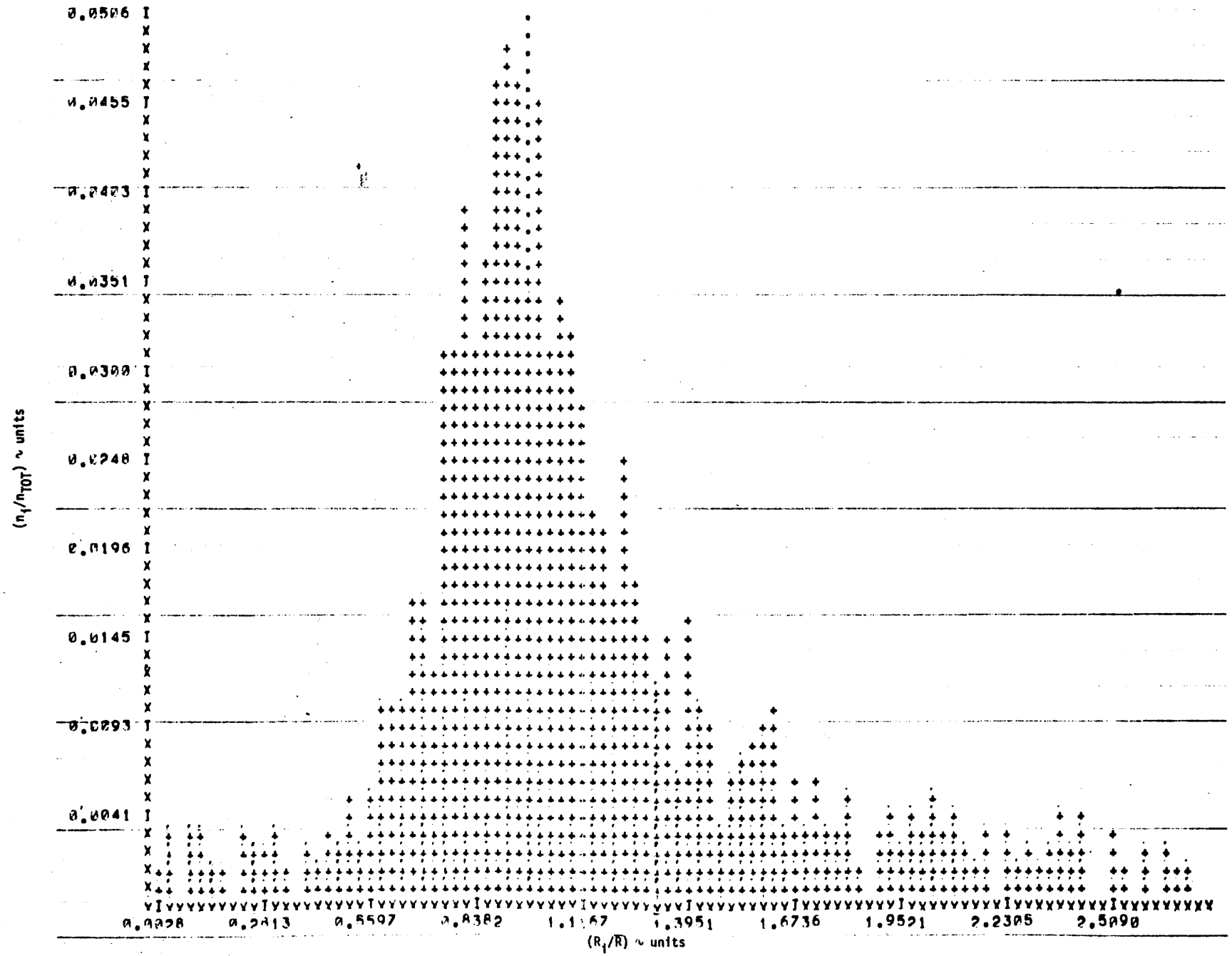

Figure 31. Probability Density of $(R/\overline{R})$ for Variation of M_f, M_x.

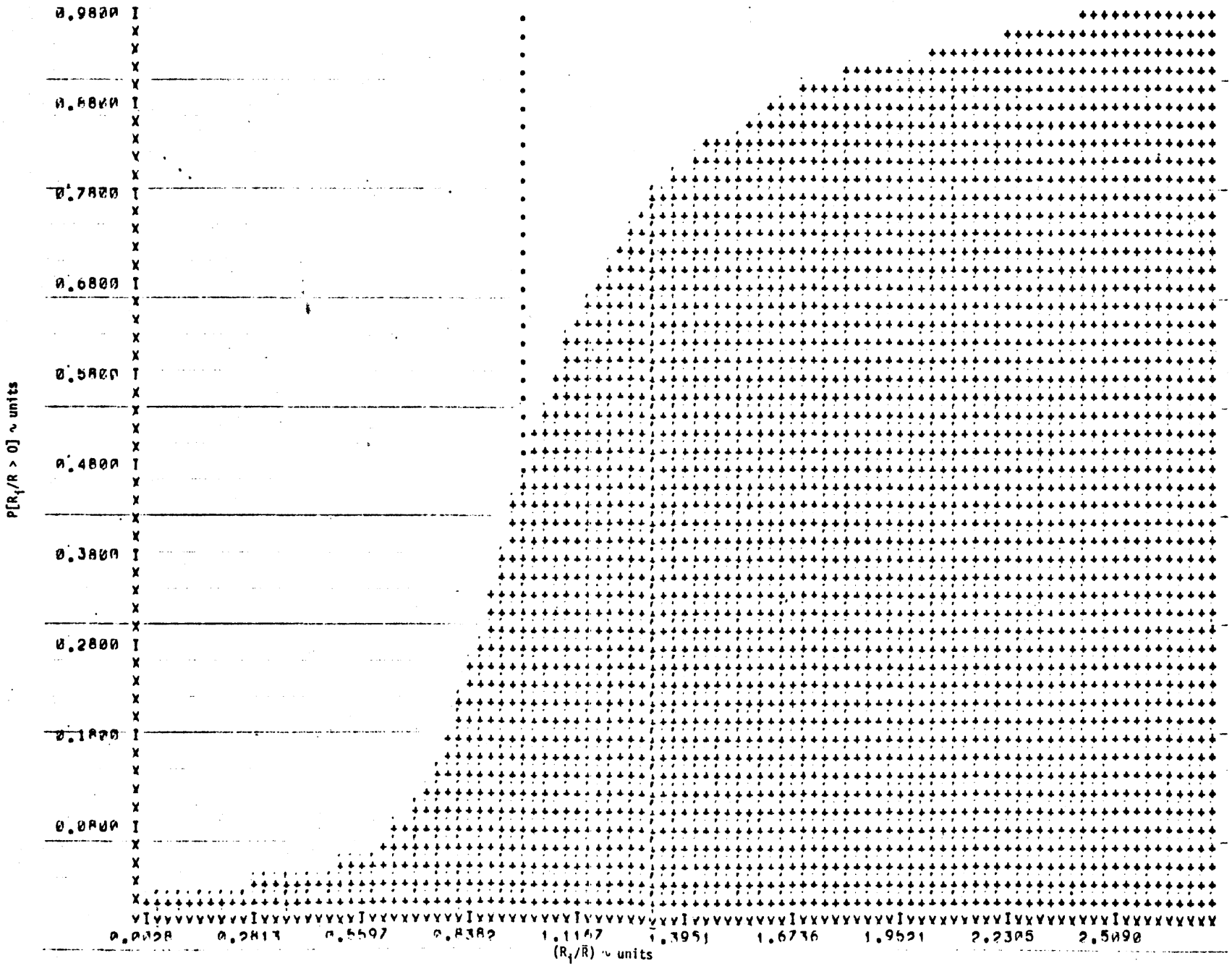

Figure 32. Cumulative Probability Distribution of $(R/\bar{R})$ for Variation of M_f, M_x.

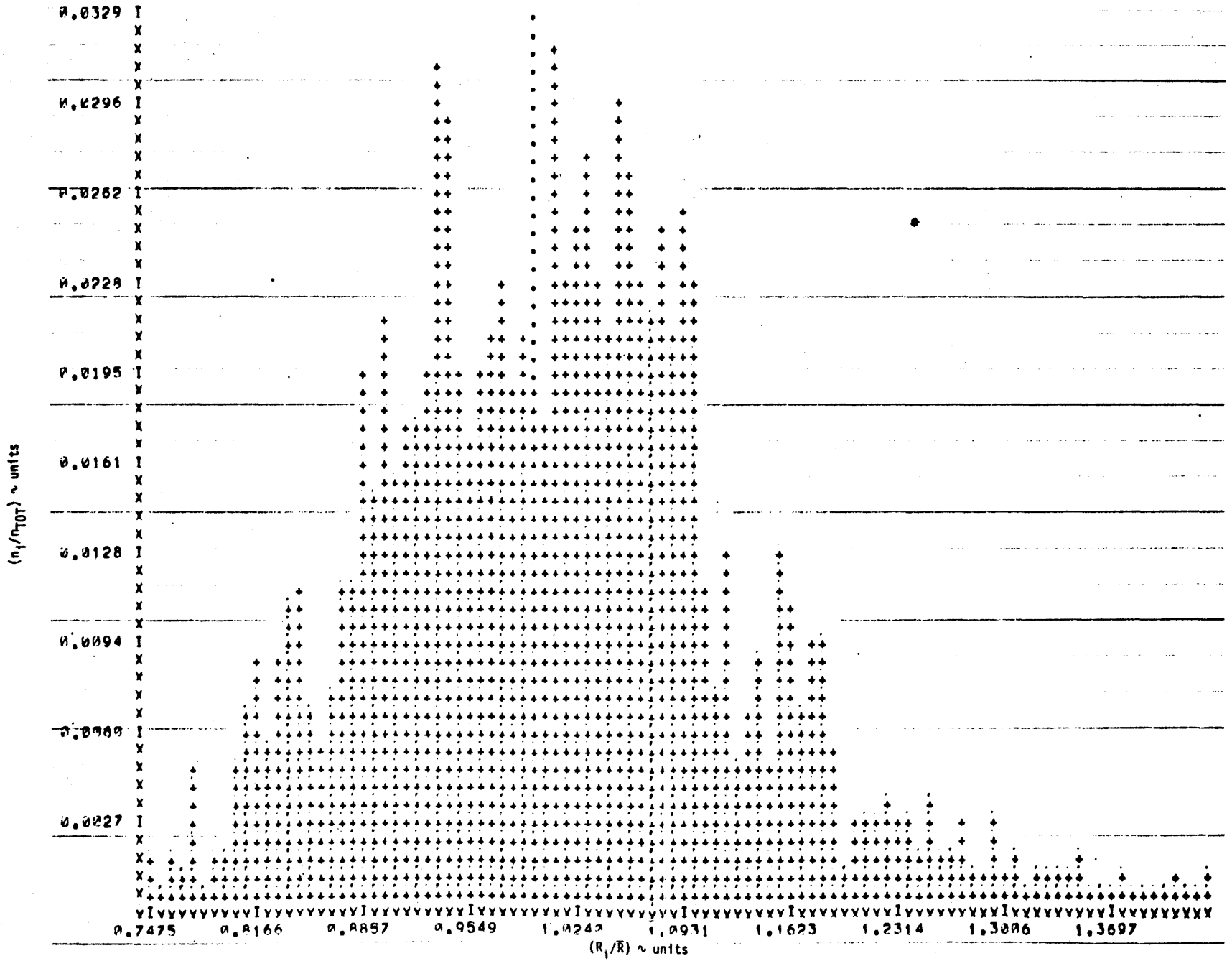

Figure 33. Probability Density of $(R/\bar{R})$ for Variation of All Weak Variables.

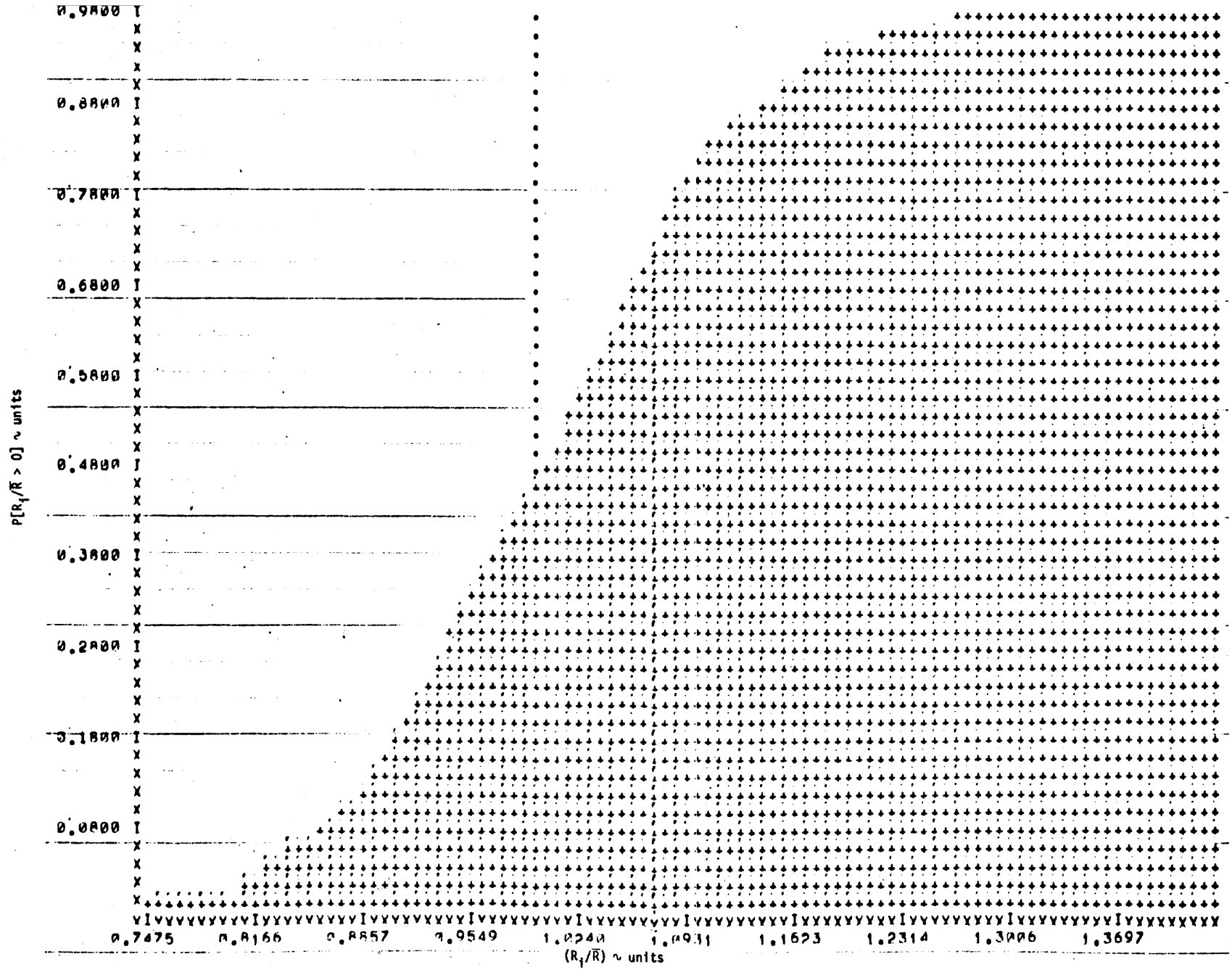

Figure 34. Cumulative Probability Distribution of $(R/\overline{R})$ for Variation of All Weak Variables.

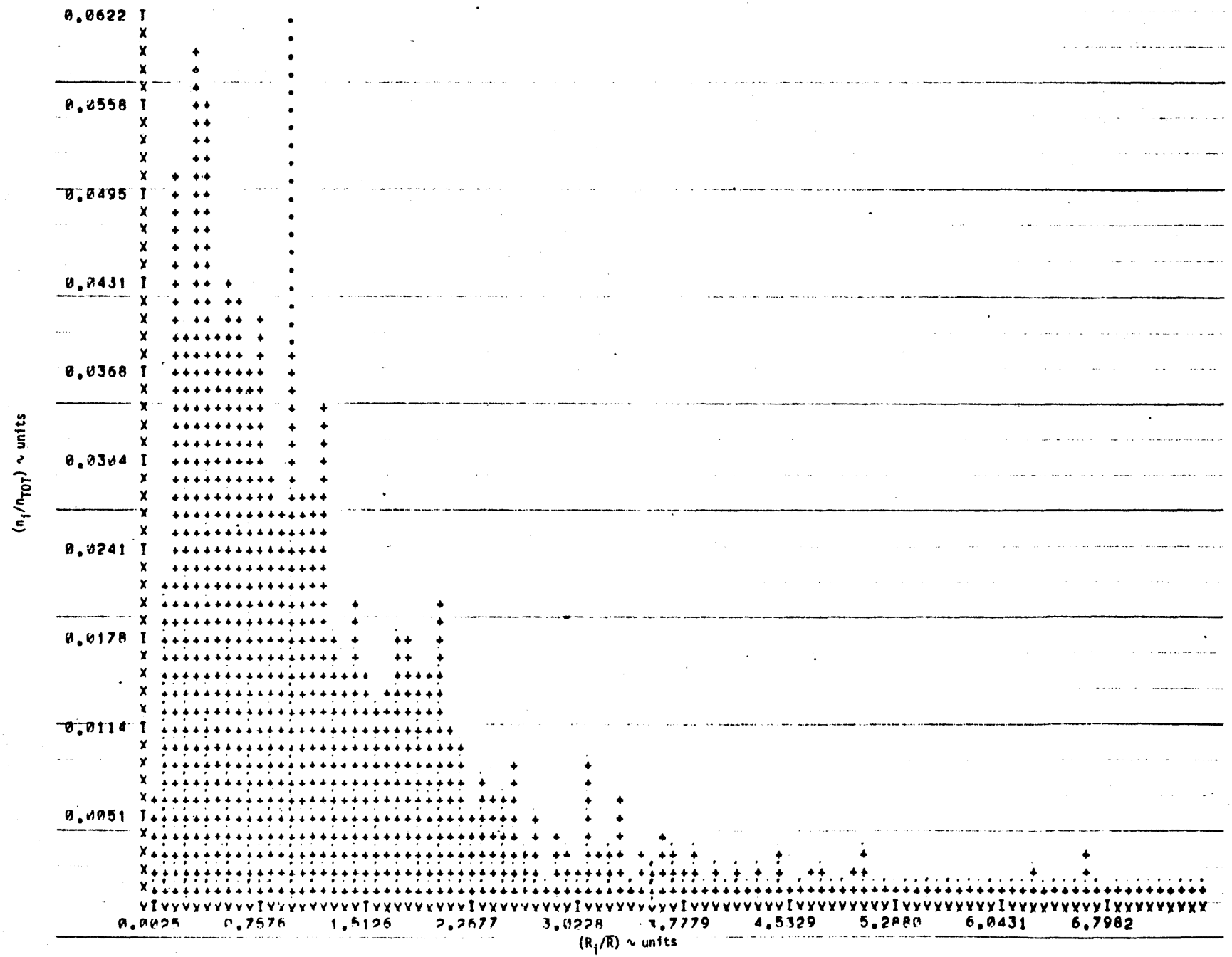

Figure 35. Probability Density of $(R/\overline{R})$ for Variation of All Strong Variables.

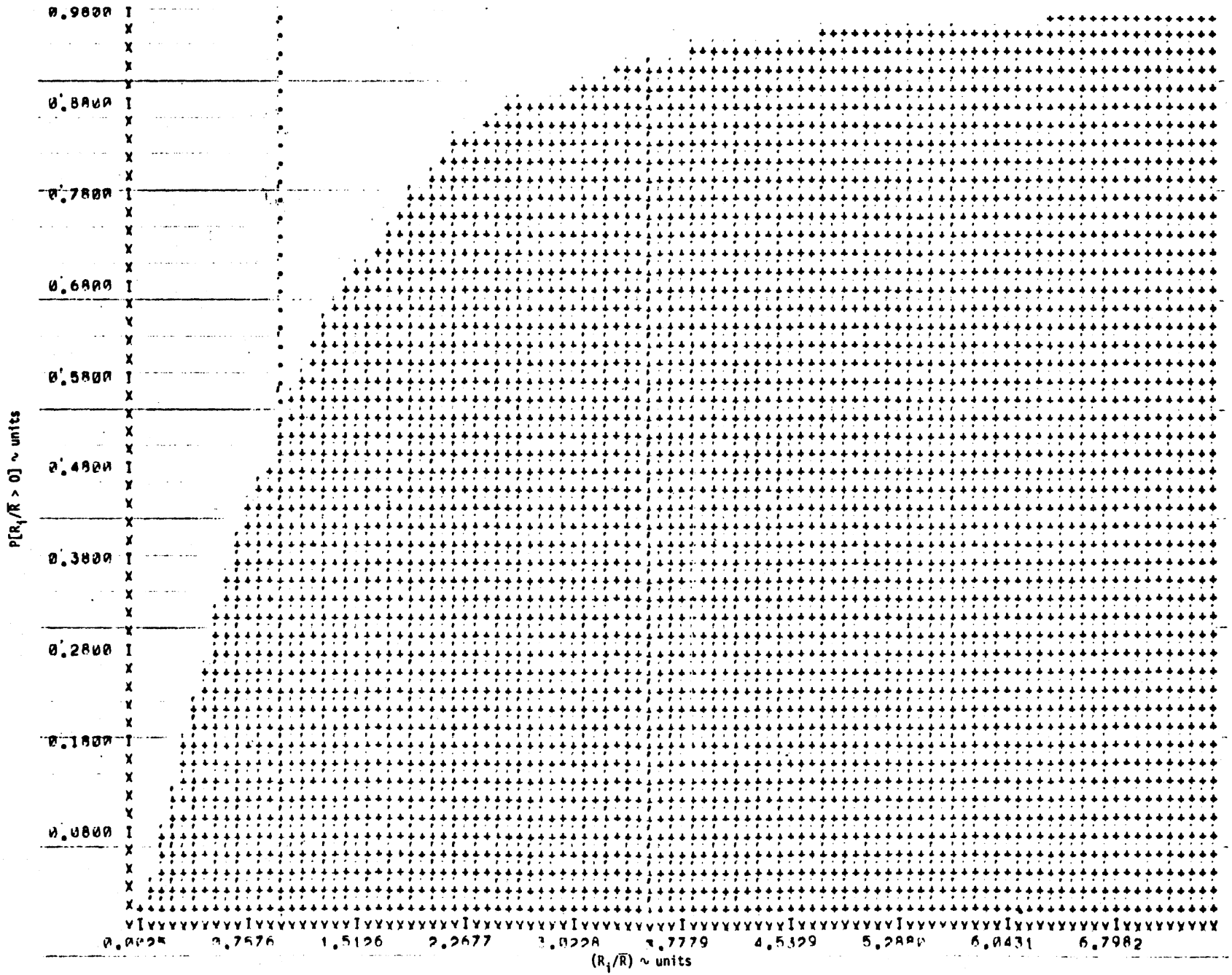

Figure 36. Cumulative Probability Distribution of $(R/\overline{R})$ for Variation of All Strong Variables.

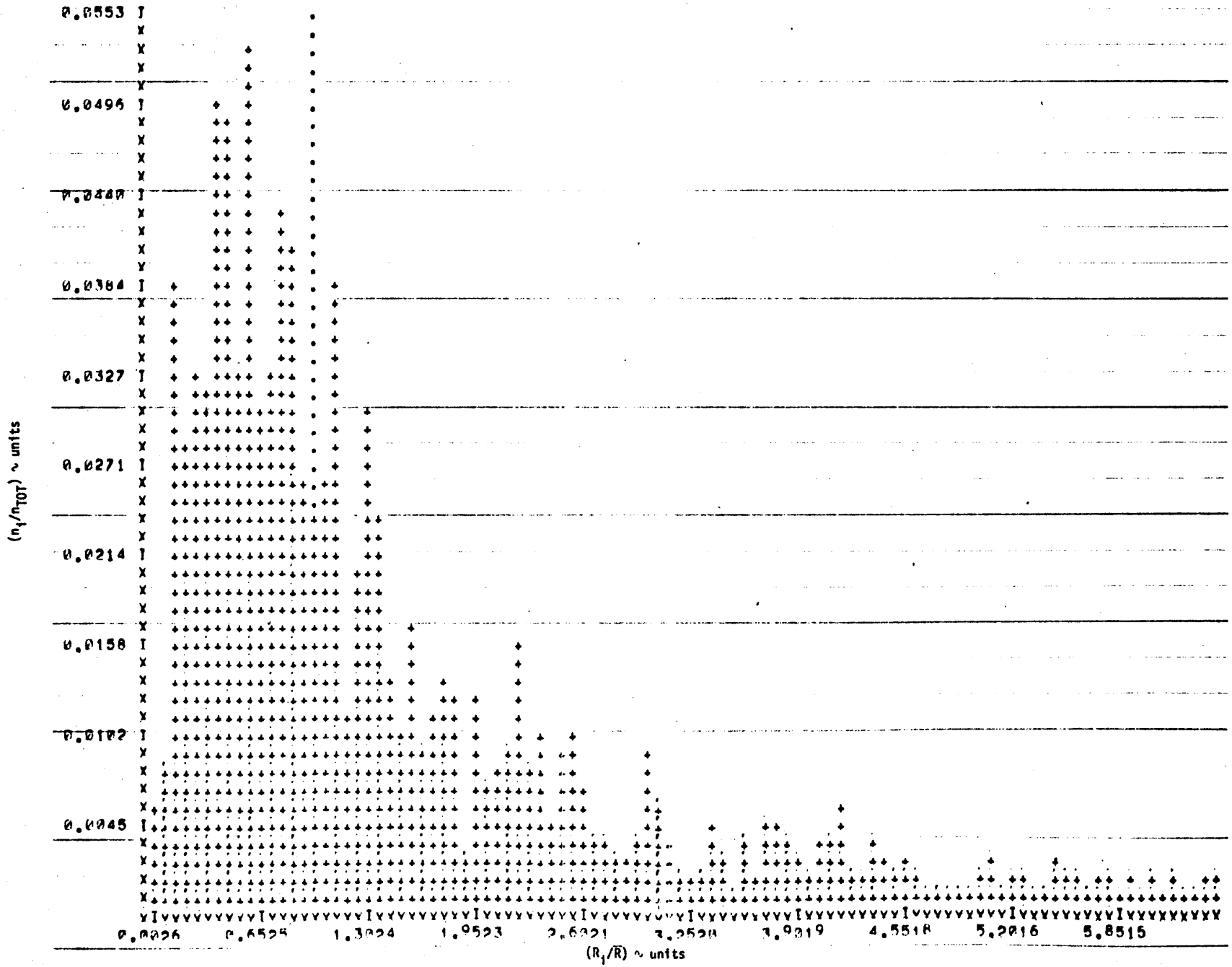

Figure 37. Probability Density of $(R/\overline{R})$ for Variation of All Variables.

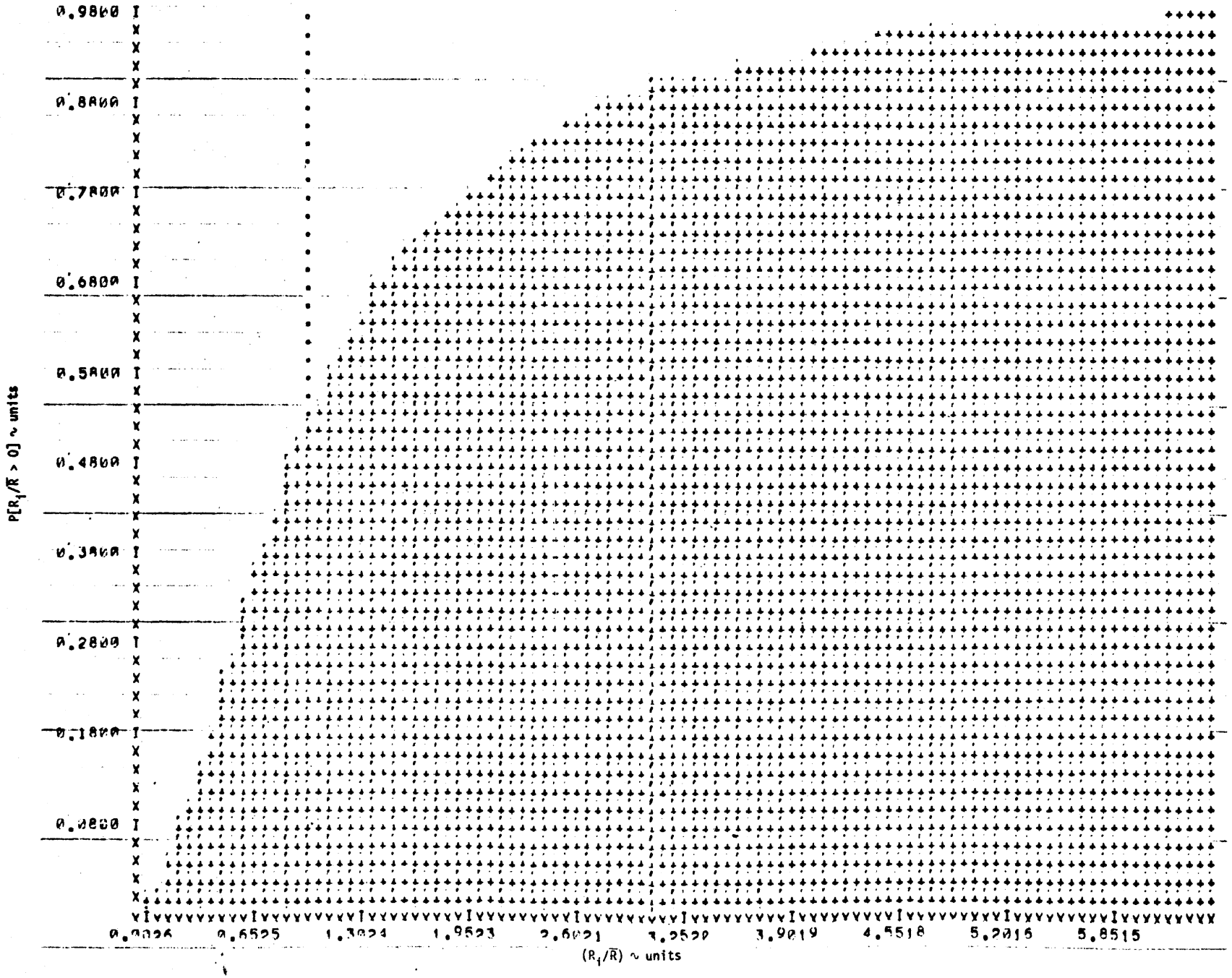

Figure 38. Cumulative Probability Distribution of $(R/\overline{R})$ for Variation of All Variables.

REFERENCES

1. Sanderlin, J.C. and Sunderson, J.M., A Simulation for Wildland Fire Management Planning Support (FIREMAN), Volume V, "Rate of Spread Model Sensitivity Analysis," MRC Report No. 7512-6-1075, October 1975.

2. Rothermel, Richard C., "A Mathematical Model for Predicting Fire Spread for Wildland Fuels,: USDA Forest Service Research Paper INT-115, 1972.